

50-286

SUMMARY OF THE TEARING STABILITY ANALYSIS OF THE  
INDIAN POINT 3 PRIMARY COOLANT SYSTEM.

Doc # 50-286  
Control # 8504050204  
Date 4/1/85 of Document:  
**REGULATORY DOCKET FILE**

— NOTICE —

THE ATTACHED FILES ARE OFFICIAL RECORDS OF THE  
DIVISION OF DOCUMENT CONTROL. THEY HAVE BEEN  
CHARGED TO YOU FOR A LIMITED TIME PERIOD AND  
MUST BE RETURNED TO THE RECORDS FACILITY  
BRANCH 016. PLEASE DO NOT SEND DOCUMENTS  
CHARGED OUT THROUGH THE MAIL. REMOVAL OF ANY  
PAGE(S) FROM DOCUMENT FOR REPRODUCTION MUST  
BE REFERRED TO FILE PERSONNEL.

DEADLINE RETURN DATE \_\_\_\_\_

\_\_\_\_\_

\_\_\_\_\_

\_\_\_\_\_

RECORDS FACILITY BRANCH

New York Power Authority Contract No. 80-121

Final Report, May 4, 1984  
Revision 1, February 7, 1985

Report Number 83-76

**SUMMARY OF THE TEARING STABILITY ANALYSIS OF THE  
INDIAN POINT 3 PRIMARY COOLANT SYSTEM**

Prepared by

**FRACTURE PROOF DESIGN CORPORATION**  
77 Maryland Plaza  
St. Louis, MO 63108

Principal Investigators

K. H. Cotter  
Paul C. Paris

Prepared for

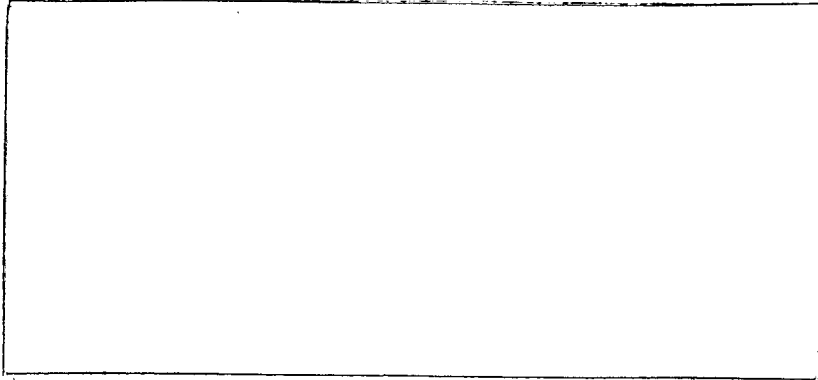
New York Power Authority  
123 Main Street  
White Plains, NY 10601

New York Power Authority Project Manager

James V. Brunetti  
Civil-Structural Department, Design and Analysis

8504050206 850401  
PDR ADDCK 05000286  
P PDR

(NON-PROPRIETARY)



**— NOTICE —**

THE ATTACHED FILES ARE OFFICIAL RECORDS OF THE DIVISION OF DOCUMENT CONTROL. THEY HAVE BEEN CHARGED TO YOU FOR A LIMITED TIME PERIOD AND MUST BE RETURNED TO THE RECORDS FACILITY BRANCH 016. PLEASE DO NOT SEND DOCUMENTS CHARGED OUT THROUGH THE MAIL. REMOVAL OF ANY PAGE(S) FROM DOCUMENT FOR REPRODUCTION MUST BE REFERRED TO FILE PERSONNEL.

DEADLINE RETURN DATE \_\_\_\_\_  
\_\_\_\_\_  
\_\_\_\_\_  
\_\_\_\_\_

RECORDS FACILITY BRANCH

## TABLE OF CONTENTS

<u>Section</u>	<u>Page</u>
1 INTRODUCTION	1-1
2 STRUCTURAL DUCTILITY CONCEPTS	2-1
2-1 Stored Elastic Energy	2-1
2-2 Structural Ductility	2-1
3 TEARING STABILITY / STRUCTURAL DUCTILITY, RESULTS AND DISCUSSION	3-1
3-1 Analysis Approach	3-1
3-2 Hot Leg Results	3-1
3-3 Cold Leg Results	3-2
3-4 Cross Leg Results	3-2
4 SSY BASED ANALYSIS	4-1
4-1 J-Integral Estimation	4-1
4-1.1 Circumferential Cracks	4-1
4-1.2 Longitudinal Cracks	4-3
4-1.3 Tearing Stability for SSY Conditions	4-3
4-1.4 Plastic Zone Instability Failure	4-4
4-2 Leak Rate Analysis	4-4
5 LEAKAGE SIZE CRACK STABILITY, RESULTS AND DISCUSSION	5-1
5-1 Primary Coolant Loop Piping System	5-1
5-1.1 System Description	5-2
5-1.2 Piping Code Structural Analysis	5-2
5-2 Leak Detectability	5-3
5-2.1 Circumferential Flaws	5-4
5-2.2 Longitudinal Flaws	5-4
5-3 Crack Stability, Level D Loads	5-5
5-3.1 Circumferential Flaws	5-5
5-3.2 Longitudinal Flaws	5-6
6 SUMMARY AND CONCLUSIONS	6-1
7 REFERENCES	7-1
APPENDIX A PROGRAM: JTIPIPE	A-1
APPENDIX B CIRCUMFERENTIAL CRACK CALCULATIONS	B-1
APPENDIX C LONGITUDINAL CRACK CALCULATIONS	C-1
APPENDIX D LEAKAGE DETECTION	D-1

THIS PAGE IS  
NON-PROPRIETARY

## Section 1

### INTRODUCTION

Beginning in July, 1980, Fracture Proof Design Corporation (FPDC) began an analysis of the New York Power Authority's (NYPA) Indian Point 3 Nuclear Power Plant for purposes of demonstrating that no asymmetric loads were applied to the reactor pressure vessel (RPV) during a postulated LOCA accident. The approach taken by FPDC was to demonstrate that even if i) upper-bound loads, that is, loads that are larger than Level D or design loads, and ii), large cracks, ranging from 60 to greater than 180° of circumferential length, were present in the reactor coolant system (RCS) piping, no instability of the cracks would occur. The conclusion of such a postulate is that no instantaneous guillotine type break could occur even under the foregoing postulated severe conditions. Thus, if no guillotine break occurs, no large LOCA loads would be present, and thus, the Indian Point 3 asymmetric load problem has been resolved.

In the summer of 1981, FPDC transmitted the results of the analysis of the Indian Point 3 RCS (1) to the USNRC. This was followed by a briefing given to the Commission's Staff in September, 1981. At the time of the briefing, the Commission indicated, verbally, that it was in agreement with the approach taken to demonstrate that no large LOCA loads could exist. But, it requested further evaluation of material properties. Thus, FPDC undertook a testing program to develop tearing

resistance data for the primary piping materials and welds, on behalf of NYPA. The test program included J-resistance curves and computation of the material tearing modulus for the wrought and cast materials and welds thereof that are in the RCS. The test program was completed in the summer of 1983 and the results (2) were forwarded to the USNRC for review.

During the period between the original submittal of the analysis of the RCS (1) and the present time, a number of criteria have been drafted for purposes of postulating pipe-breaks in nuclear piping using fracture mechanics methods. This activity culminated with the USNRC publishing a draft criteria (3) in November, 1983. Between 1981 and the present, developments in analysis methodology and concepts were being made. These included the work of Paris and Cotter (4) on the concept of structural ductility.

It is the intent of this summary document to re-evaluate the results of the original analysis (1) by incorporating the material resistance data developed in the test program (2), to compare the analysis with the proposed NRC criteria (3), and finally, to demonstrate the applicability of the new structural ductility (4) concepts.

## Section 2

### STRUCTURAL DUCTILITY CONCEPTS

The fundamental concepts involved in structural ductility arguments were presented by Paris and Cotter (4) and Paris (5) and are reviewed in this section to acquaint the unfamiliar reader.

#### 2-1 STORED ELASTIC ENERGY

Earlier arguments by Nathan Newmark showed that to insure sufficient structural ductility, it was necessary to show that a structure could absorb (up to) twice its stored elastic energy by a plastic energy dissipation mechanism. Paris and Cotter (4) applied this concept to problems involving the integrity of nuclear piping and related the Newmark requirement to the tearing modulus (6) approach.

\* \* \* \* PROPRIETARY DATA OMITTED \* \* \* \*

#### 2-2 STRUCTURAL DUCTILITY

The foregoing section, describing the absorption of stored elastic energy is only one of two portions of the structural ductility arguments presented by Paris and Cotter (4). Following their arguments, it is

noted that the requirement of Equation 2-7 is based on a global energy dissipation requirement. The portion remaining is that of a local requirement. In structural analyses involving nuclear piping systems, the local requirement is met by determining the value of the applied J-integral, at the crack section, due to local loading conditions. The value for  $J_{app}$  is readily computed using one or more methods. For the purpose of this analysis, the JTPIPE computer program (8) was used. By so doing, it is found that the total J at the crack section is equal to

\* \* \* \* PROPRIETARY DATA OMITTED \* \* \* \*

if structural ductility requirements are to be met. An additional requirement is that, to insure crack stability, the value of the applied tearing modulus,  $T_{app}$ , must satisfy

$$\eta T_{app} < T_{mat} \quad (2-9)$$

where  $T_{app}$  is computed by use of JTPIPE or by similar schemes,  $T_{mat}$  is the value of the material tearing modulus, corresponding to the value of  $J_{app}$  given in Equation 2-7 and  $\eta$  is the Newmark factor,

\* \* \* \* PROPRIETARY DATA OMITTED \* \* \* \*

Thus, the second requirement to insure structural ductility is satisfaction of Equation 2-9, which is simultaneously subject to the  $J_{app}$  being computed in accordance with Equation 2-7. In other words, the  $J_{app}$  and  $T_{app}$ , as developed in Equation 2-8 and 2-9, must be adequately within the stable region of a J-T stability diagram.

## Section 3

### RESULTS

It was necessary to re-analyze the Indian Point 3 RCS because of the development of the new material property data (2), the development of new bounding loads as described below, and the development of structural ductility concepts (4).

#### 3-1 ANALYSIS APPROACH

This sub-section describes the analytical methods used for analyzing the RCS.

\* \* \* \* PROPRIETARY DATA OMITTED \* \* \* \*

#### 3-2 HOT LEG RESULTS

An isometric view of the RCS is shown in Figure 3-3a, the hot leg of the RCS connects the RPV to the steam generator (SG). This is shown in elevation view in Figures 3-3b (OMITTED AS PROPRIETARY) and 3-3c, based on measurements taken at the Indian Point 3 site (11),

\* \* \* \* PROPRIETARY DATA OMITTED \* \* \* \*

The total value of  $J_{app}$  is represented by the horizontal bar at the limit

of the vertical line as shown in Figures 3-5 thru 3-7. Using this approach, and material data based on deformation theory J,  $J_d$ , stability of the hot leg was proven unconditionally.

### 3-3 COLD LEG RESULTS

The plan view of the RCS is shown in Figure 3-8.

\* \* \* \* PROPRIETARY DATA OMITTED \* \* \* \*

Stability of the cold leg was demonstrated based on tearing stability and structural ductility as shown in Figures (OMITTED AS PROPRIETARY).

### 3-4 CROSS LEG RESULTS

The cross leg is shown in Figure 3-16a and its idealization in

\* \* \* \* PROPRIETARY DATA OMITTED \* \* \* \*

The results, using deformation theory J for the material resistance, are shown in Figures 3-17 through 3-19. Again, these represent results for 60, 120, and 180 degrees, respectively. Stability is again indicated even with these unduly conservative assumptions on loading.

+ + + + NOTE: ALL PROPRIETARY FIGURES ARE OMITTED + + + +

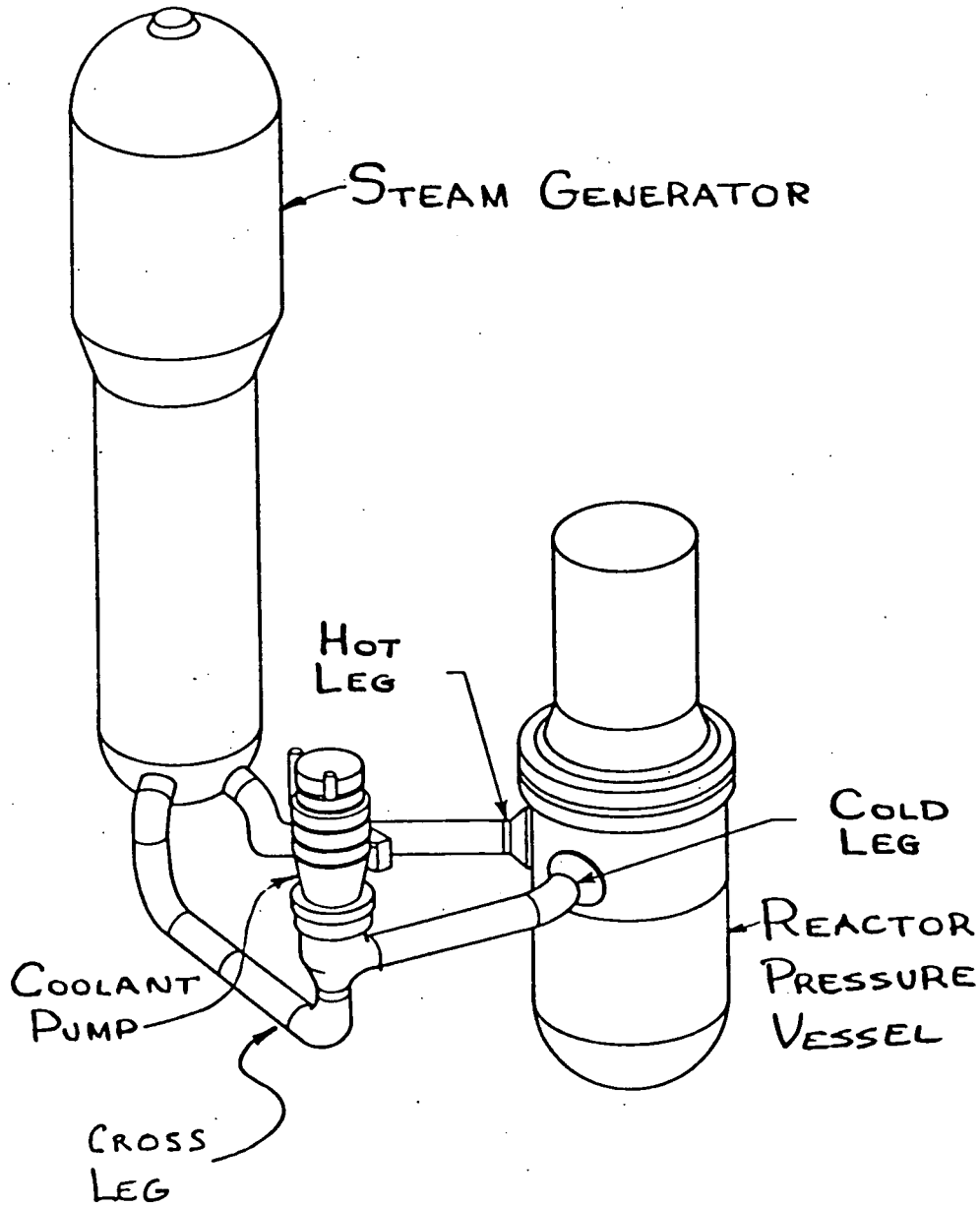
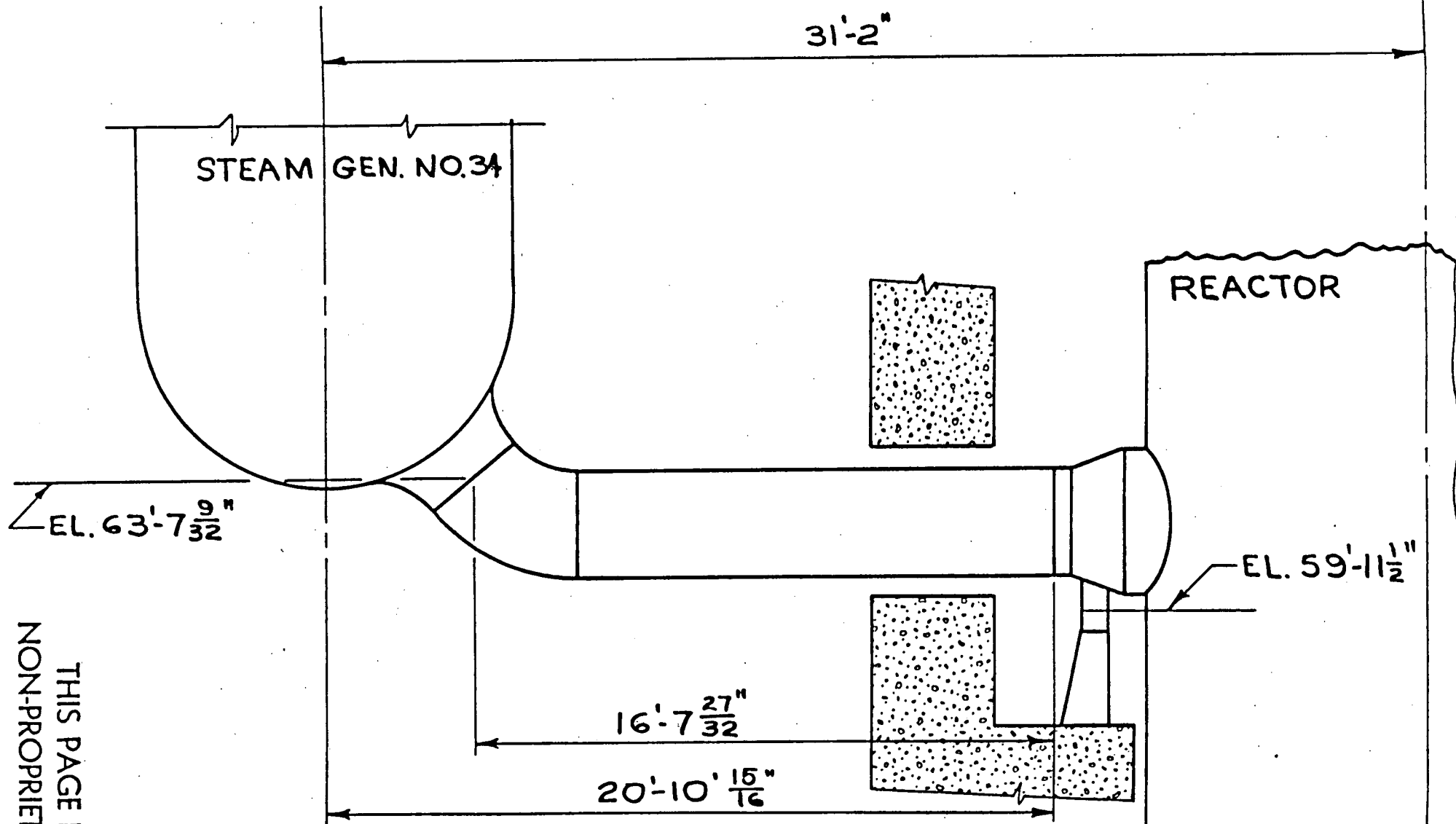


Figure 3-3a Isometric View of Indian Point 3 RCS

THIS PAGE IS  
NON-PROPRIETARY



THIS PAGE IS  
NON-PROPRIETARY

SECTION A-A (HOT LEG)  
FROM DWG NO 202101

Figure 3-3c

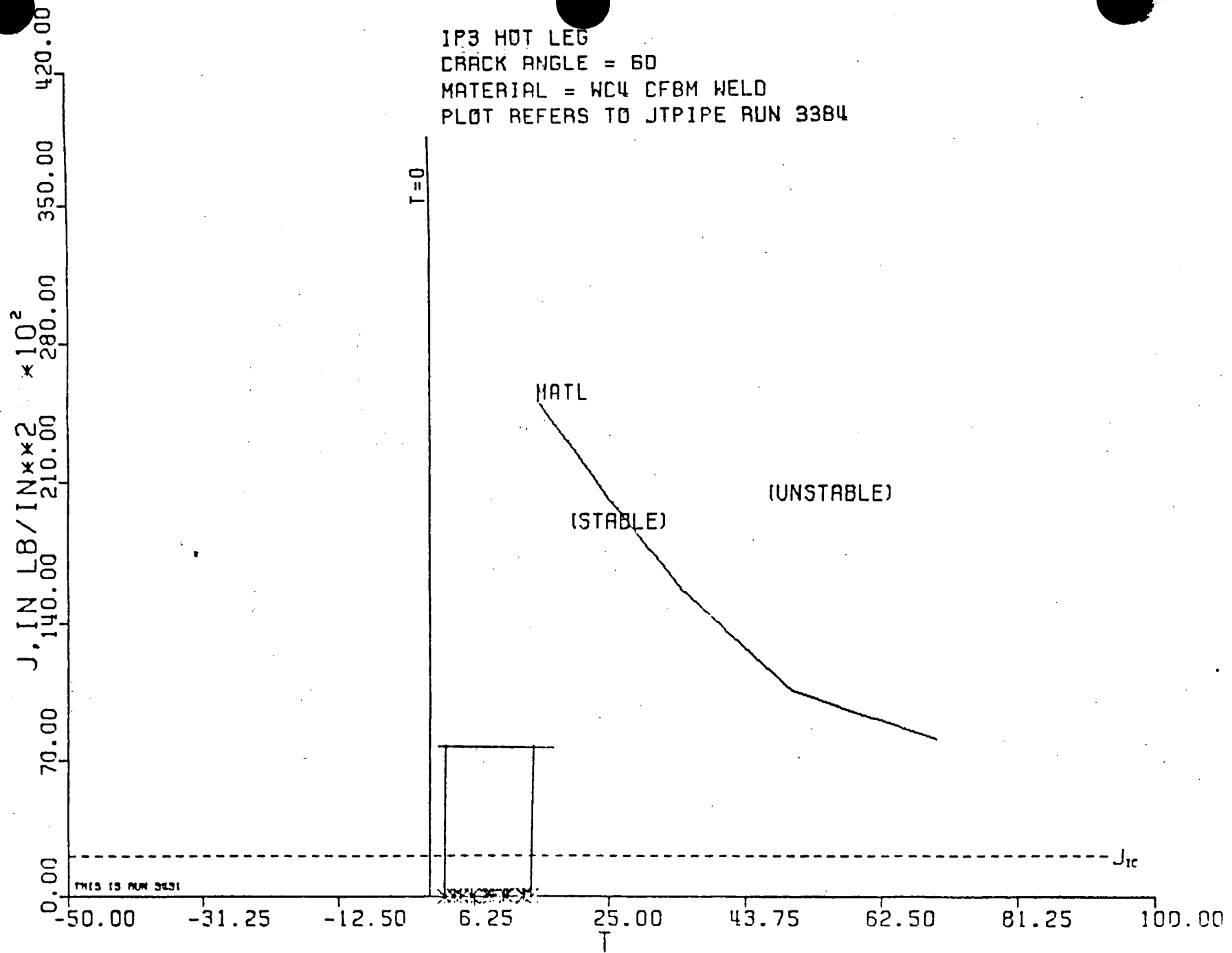


Figure 3-5 Hot Leg J-T Stability Diagram,  $2\theta = 60^\circ$ ,  $J_d$

IP3 HOT LEG  
 CRACK ANGLE = 120  
 MATERIAL = WC4 CF8M WELD  
 PLOT REFERS TO JPIPE RUN 3385

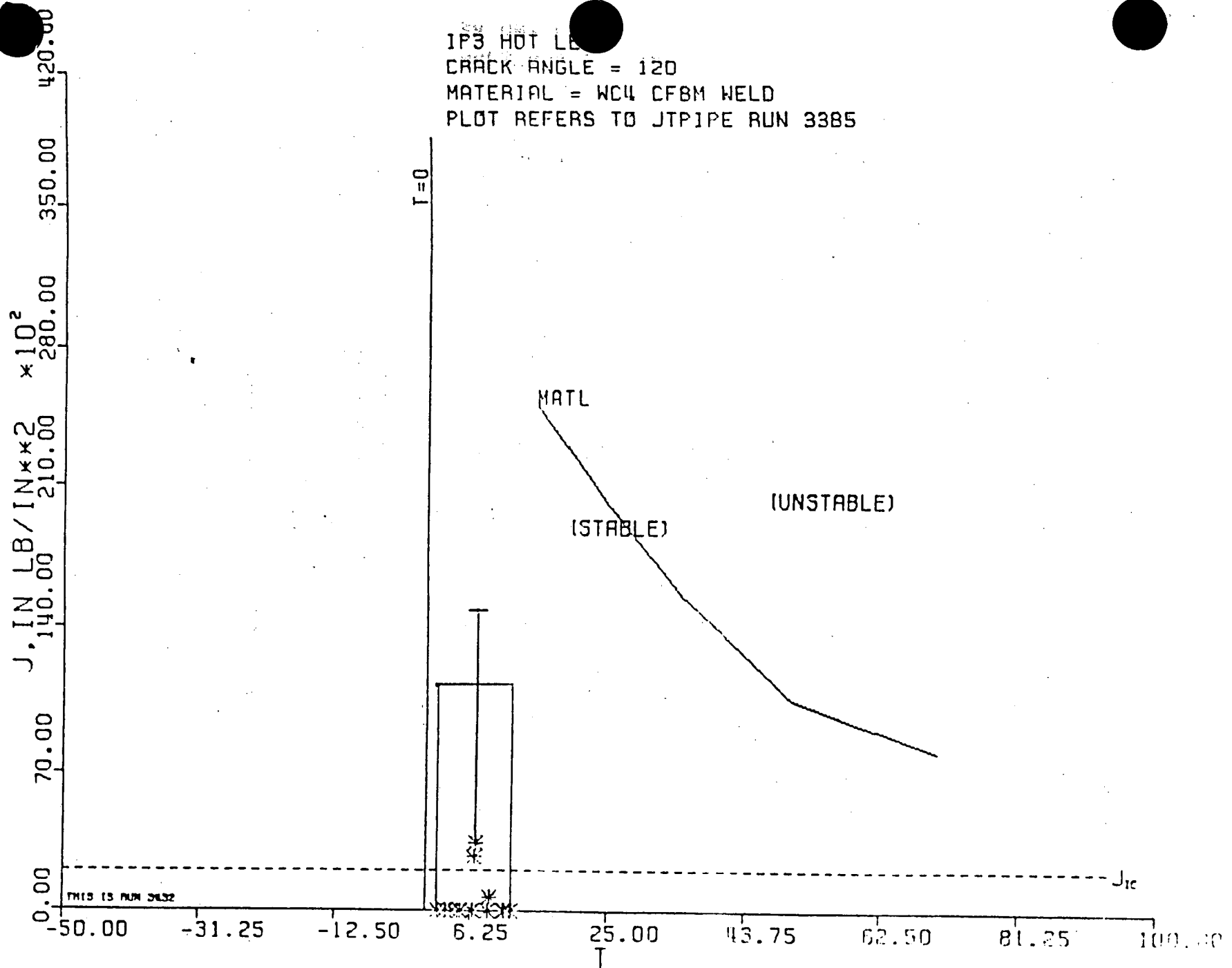


Figure 3-6 Hot Leg J-T Stability Diagram,  $2\theta = 120^\circ$ ,  $J_d$

IP3 HOT LEG  
 CRACK ANGLE = 180  
 MATERIAL = WC4 CF8M WELD  
 PLOT REFERS TO JPIPE RUN 3387

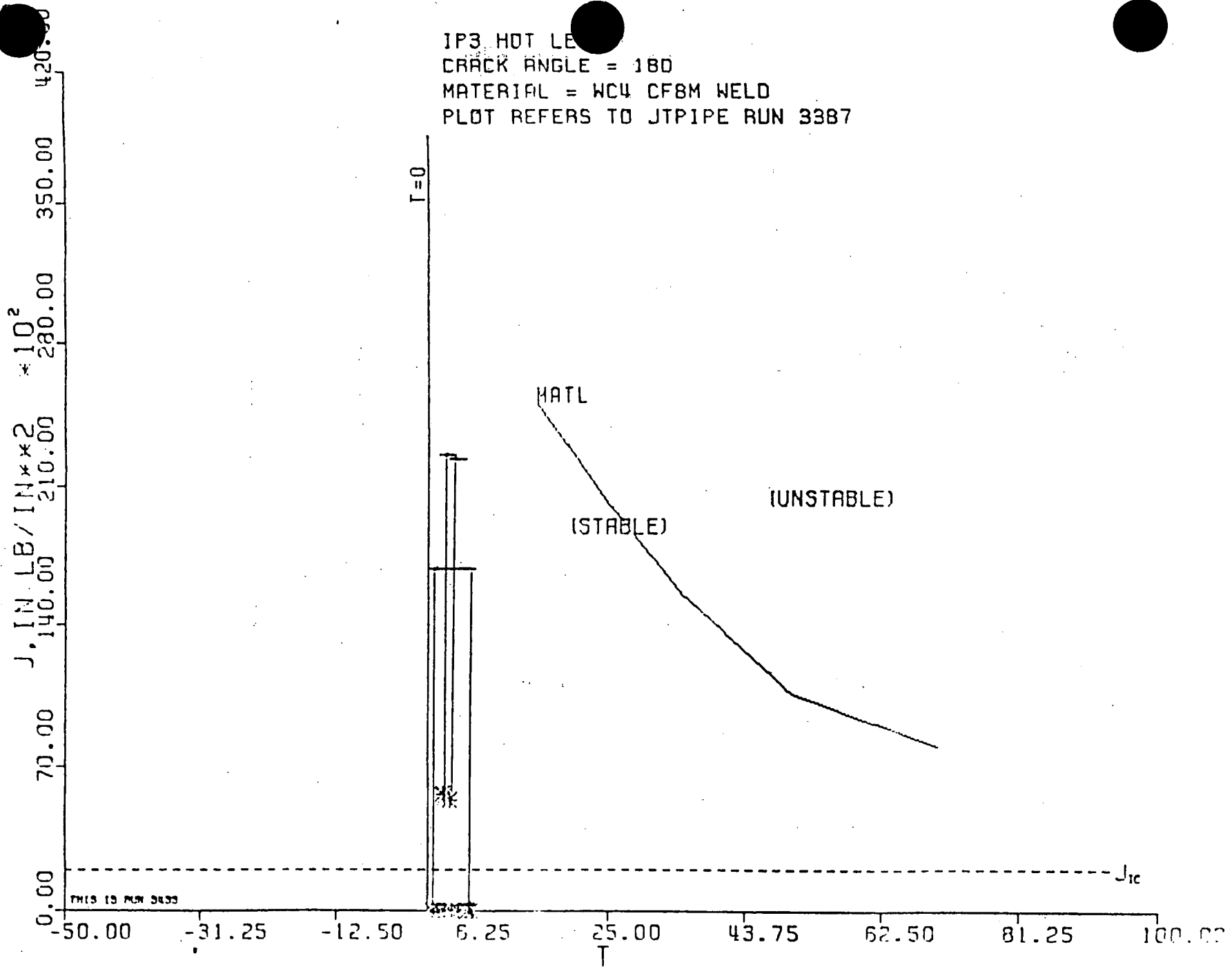


Figure 3-7 Hot Leg J-T Stability Diagram,  $2\theta = 180^\circ$ ,  $J_d$

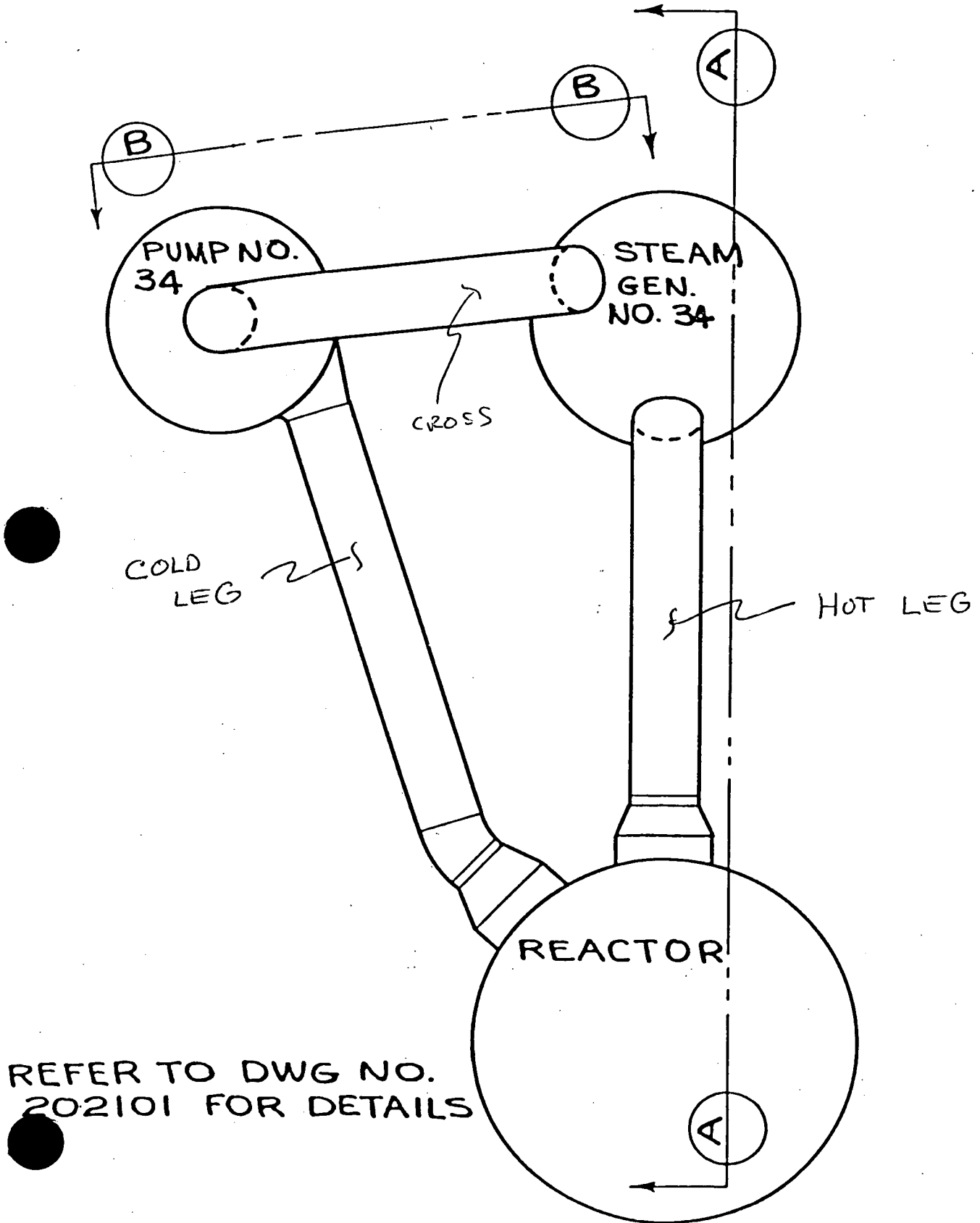
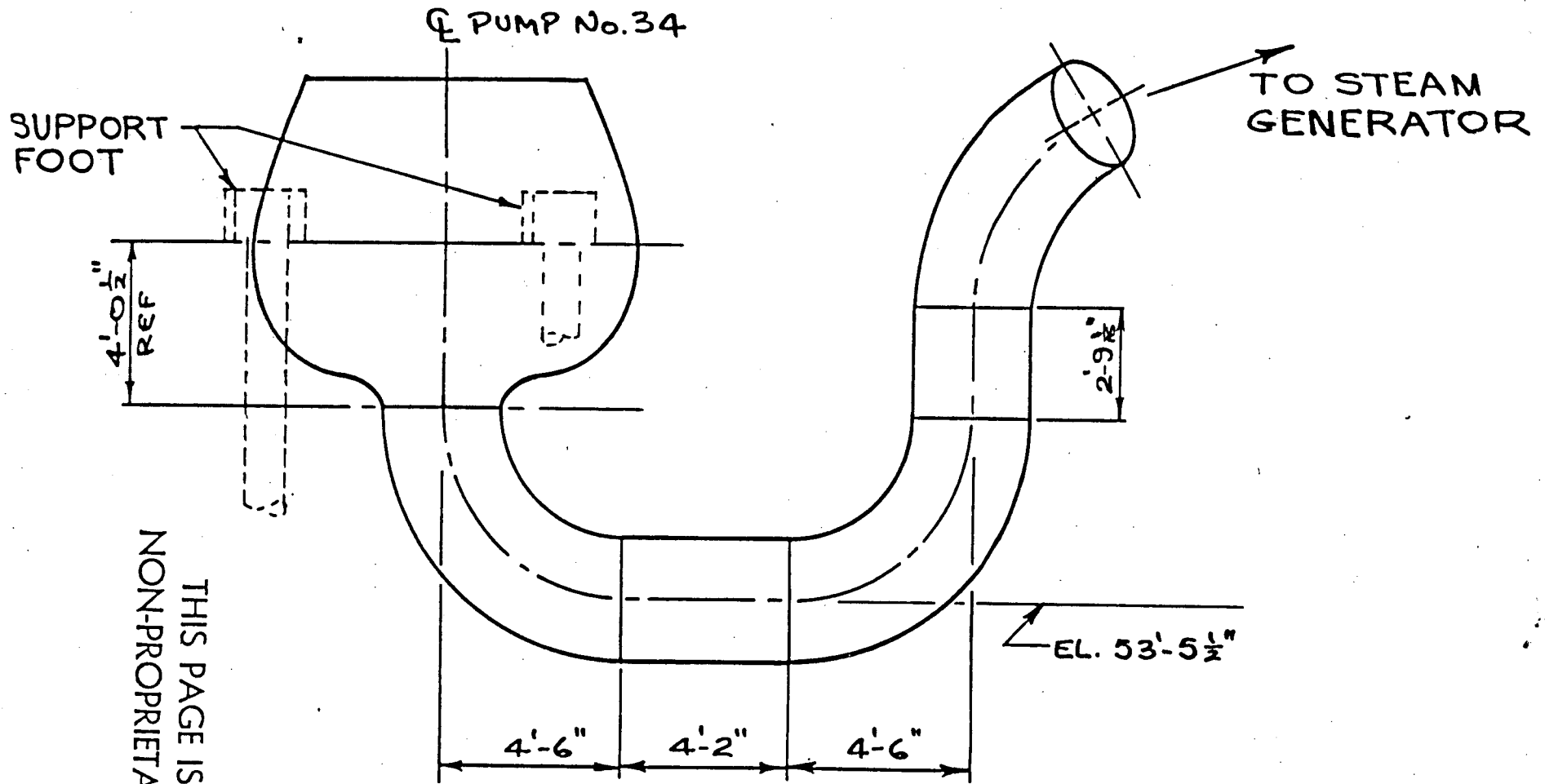


Figure 3-8 Bottom View Primary Coolant System



THIS PAGE IS  
 NON-PROPRIETARY

SECTION B-B (CROSS LEG)  
 FROM DWG NO 202101

Figure 3-16a

IP3 CROSS LEG  
 CRACK ANGLE = 60  
 MATERIAL = WC4 CF8M WELD  
 PLOT REFERS TO JPIPE RUN 3442

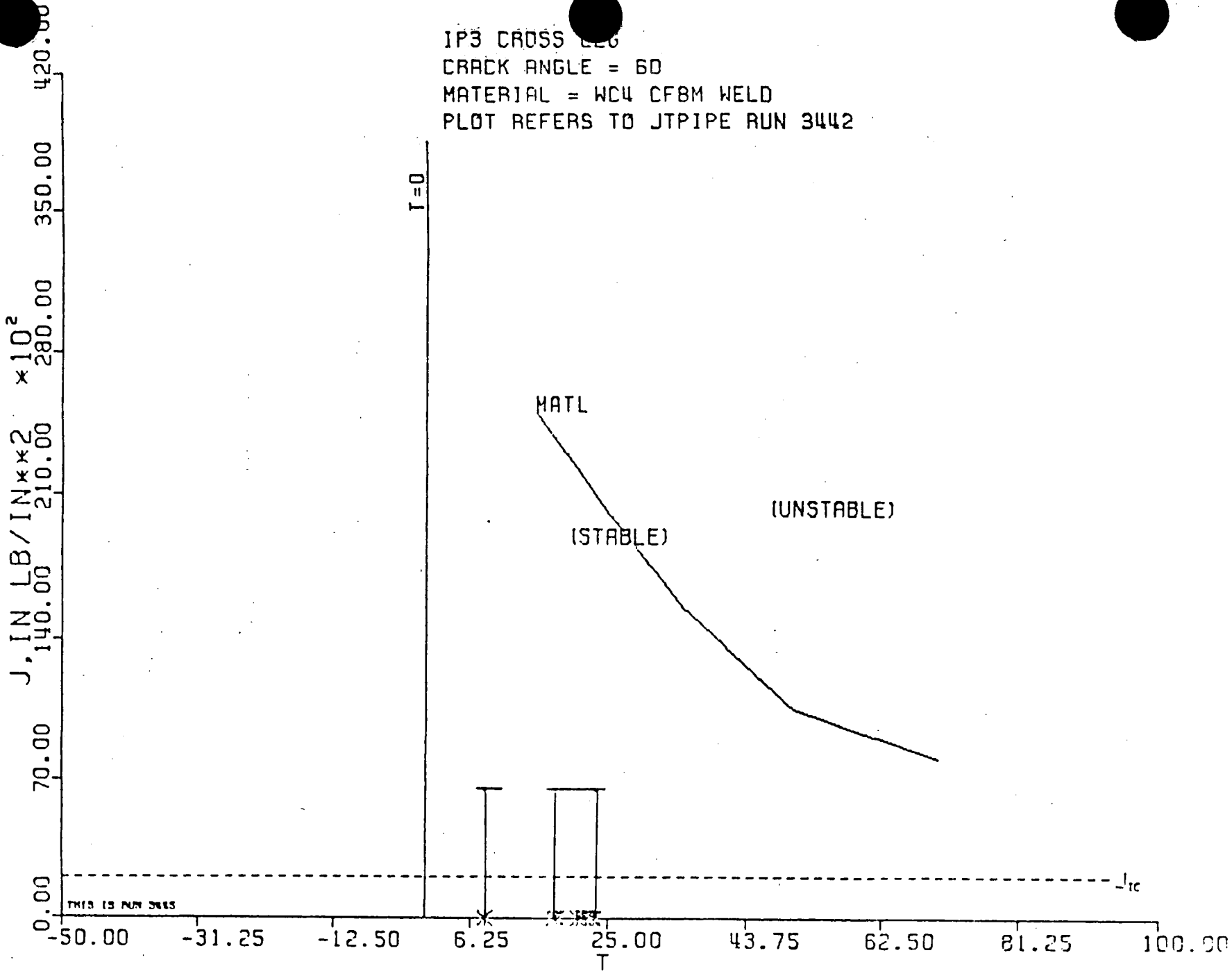


Figure 3-17 Cross Leg J-T Stability Diagram,  $2\theta = 60^\circ, J_d$

IP3 CROSS LEG  
 CRACK ANGLE = 120  
 MATERIAL = WC4 CF8M WELD  
 PLOT REFERS TO JPIPE RUN 3443

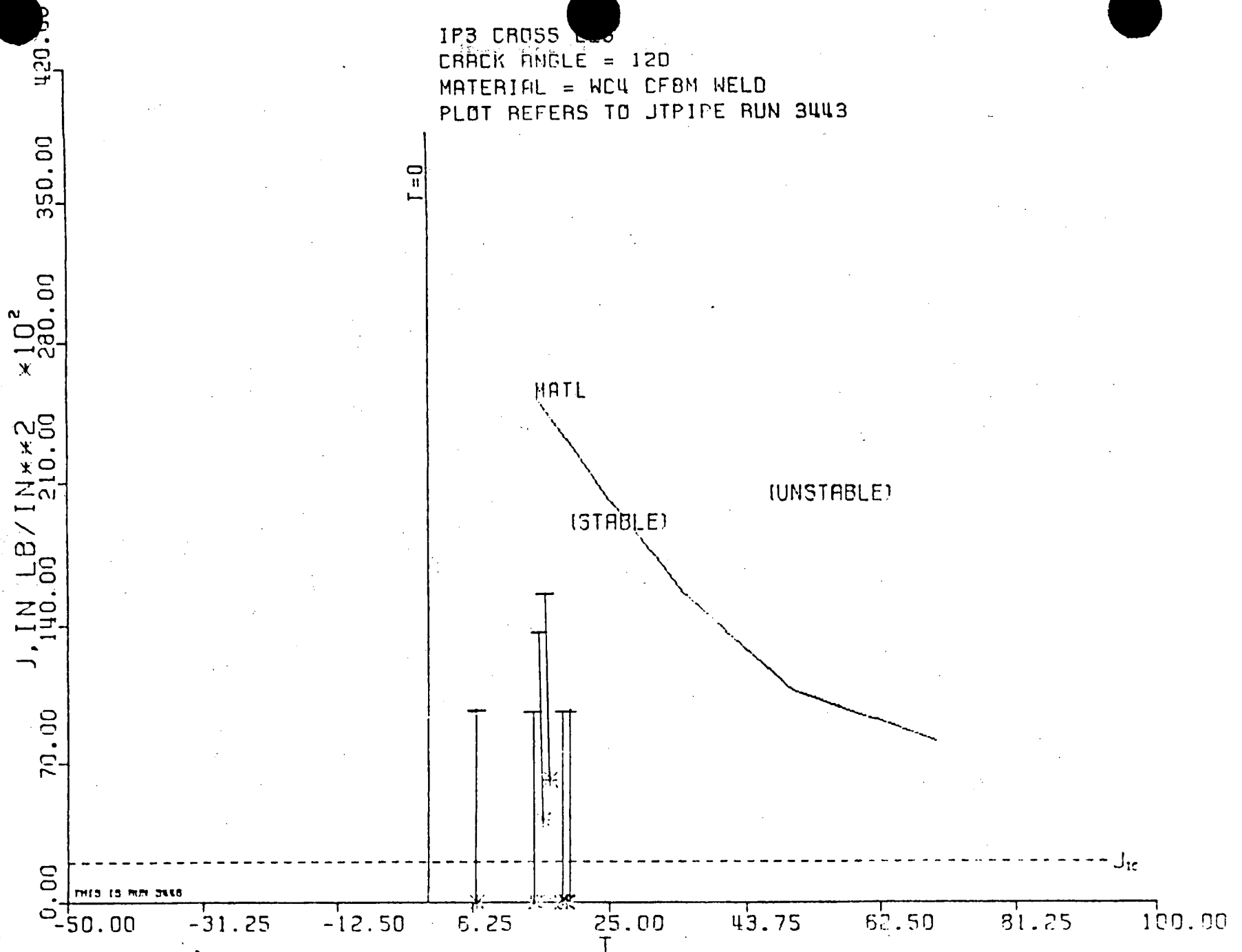


Figure 3-18 Cross Leg J-T Stability Diagram,  $2\theta = 120^\circ$ ,  $J_d$

IP3 CROSS LEG  
 CRACK ANGLE = 180  
 MATERIAL = WC4 CF8M WELD  
 PLOT REFERS TO JPIPE RUN 3444

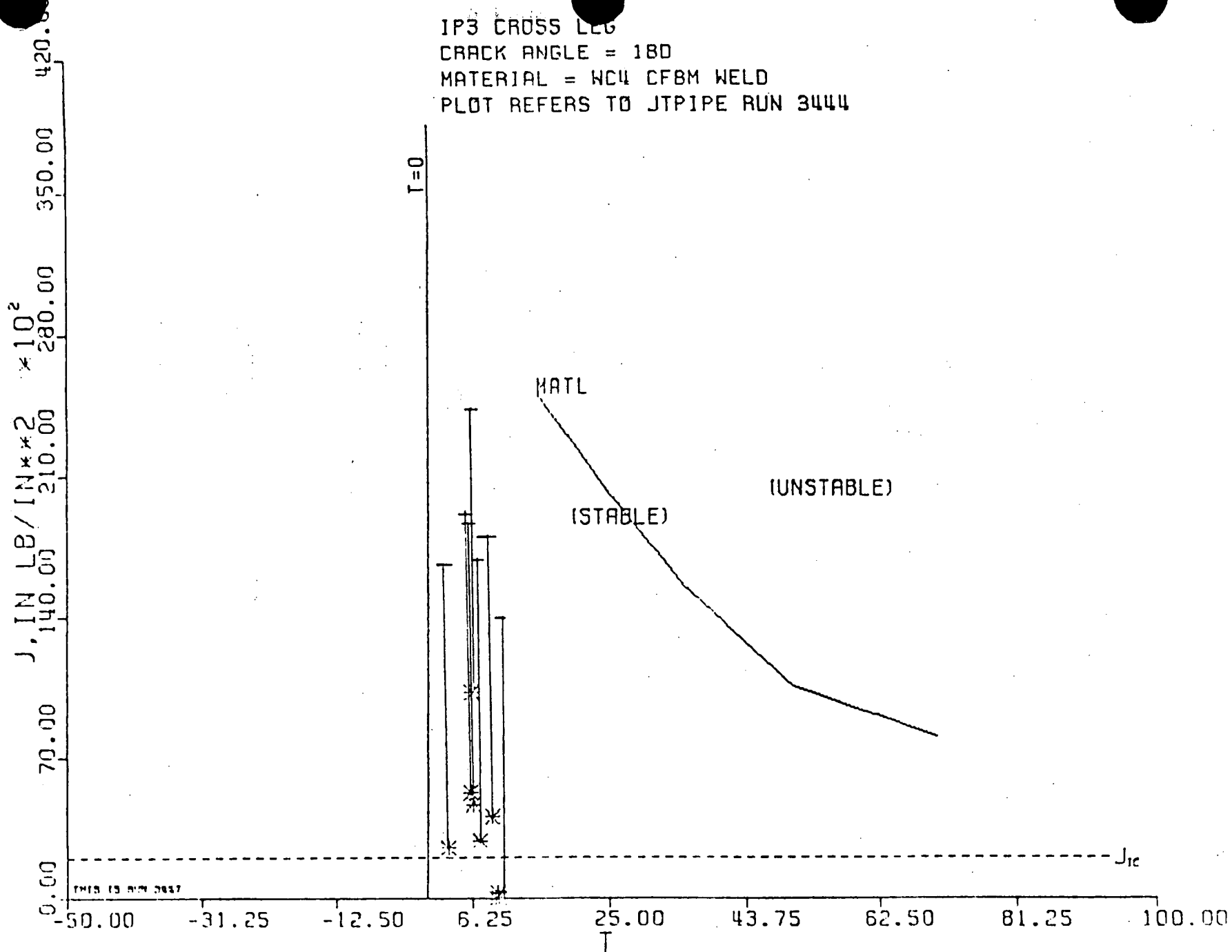


Figure 3-19 Cross Leg J-T Stability Diagram,  $2\theta = 180^\circ$ ,  $J_d$

## Section 4

### SSY BASED ANALYSIS

The stability of leakage size cracks can be determined, in general, by the use of methods based on the small-scale yielding theories of fracture mechanics.

#### 4-1 J-INTEGRAL ESTIMATION

For the ssy regime, the J-integral,  $J_{app}$ , can be estimated using the relation

$$J_{app} = K_I^2/E' \quad (4-1)$$

where  $E'=E$  for plane stress,  $E'=E/(1-\mu^2)$  for plane strain,  $K_I$  is the opening mode plastic zone corrected stress-intensity factor,  $E$  is the elastic modulus and  $\mu$  is Poisson's ratio.

##### 4-1.1 Circumferential Cracks

For circumferential cracks, the  $K_I$  consists of contributions from three types of loads: axial load, bending moment and membrane stress due to pressure. The  $K_I$  due to pressure loading,  $K_m$ , was obtained by utilizing the solutions from Reference (12), giving

$$K_m = \sigma_m \sqrt{\pi R \theta} F_m \quad (4-2)$$

THIS PAGE IS  
NON-PROPRIETARY

where  $\sigma_m$  is the membrane stress (axial) and  $F_m$  is a non-dimensional shell correction factor that depends upon the length of the crack and the geometrical dimensions of the shell.

The  $K_I$  due to the applied axial tension load is

$$K_t = \sigma_t \sqrt{\pi R \theta} F_t \quad (4-3)$$

where  $F_t$  depends upon the same parameters as  $F_m$ . The function  $F_t$  can be derived from the recent work of Erdogan and Delale(13). FPDC has developed its own approximate, but conservative, expression for  $F_t$  which was used in this study.  $\sigma_t$  is the stress (tension) due to the axial load

$F_{ax}$

$$\sigma_t = F_{ax} / (2\pi R t) \quad (4-4)$$

Similar to the tension loading case, FPDC had previously developed an estimate of  $K$  for the externally applied bending load; and the  $K$  due to this loading is

$$K_b = \sigma_b \sqrt{\pi R \theta} F_b \quad (4-5)$$

where  $F_b$  is a correction factor for a circumferential crack in a shell subjected to a bending load.  $\sigma_b$  is the maximum bending stress due to the external moment,  $M$ ,

$$\sigma_b = M/Z \quad (4-6)$$

THIS PAGE IS  
NON-PROPRIETARY

where  $Z$  is the elastic section modulus. The total  $K_I$  due to these three types of loading is

$$K_I = K_m + K_t + K_b \quad (4-7)$$

Equations (4-7) and (4-1), when combined together, give the functional form for  $J_{app}$ .

#### 4-1.2 Longitudinal Cracks

The computation of crack stability for longitudinal flaws is based on plastic zone corrected stress-intensity factor solutions (14). For a longitudinal through crack in a pipe

$$K = \sigma_h \sqrt{\pi c} F(\lambda) \quad (4-8)$$

where  $\sigma_h$  is the hoop stress,  $c$  is half the crack length,  $\lambda = c/\sqrt{Rt}$  and the shell correction term  $F(\lambda) = (1 + 1.3\lambda^2)^{-.5}$  for  $\lambda < 1$  and  $F(\lambda) = .5 + .9\lambda$  for  $1 < \lambda < 4.45$ .  $J_{app}$  can be found as before from Equation (4-1).

#### 4-1.3 Tearing Stability for SSY Conditions

The form for  $T_{app}$  can be found by differentiating the equation for  $J_{app}$  following Equations (4-1) and (4-7) or (4-8), with respect to crack length, giving

$$T_{app} = \frac{dJ_{app}}{da} \frac{E}{\sigma_o^2} \quad (4-9)$$

THIS PAGE IS  
NON-PROPRIETARY

Then, using Equations (2-2) through (2-4), the stability of the crack can be determined.

#### 4-1.4 Plastic Zone Instability Failure

Vasquez and Paris(14) have shown that situations exist in which the gradient with respect to the crack size of the elastic stress field at the tip of the crack becomes sufficiently large that the plastic zone cannot maintain stable static equilibrium and plastic zone instability occurs, followed by the propagation (or unstable extension) of the crack. This mode of unstable extension is called a "plastic zone instability failure" or PZIF). The functional form of the PZIF criterion is given by

$$K_{pzif}^2 = 2\pi\sigma_0^2 c_{eff}/P_z \quad (4-10)$$

where  $P_z = 1 + 2\lambda F'/F$ , and  $c_{eff}$ ,  $\lambda$  and  $F(\lambda)$  are the plastic zone corrected terms described in Equation (4-8).

#### 4-2 LEAK RATE ANALYSIS

The estimate of the leak rate for various cracks was based upon the LFM based methods given in Reference (15). In general, the leak rate depends upon the applied stress and crack length. Thus, the calculation of leak rate necessitates the development of a fluid flow model for fluid leaking through a crack. It also requires consideration of the thermodynamics of the flow and the surface roughness of the crack.

THIS PAGE IS  
NON-PROPRIETARY

## Section 5

### LEAKAGE SIZE CRACK STABILITY, RESULTS AND DISCUSSION

The theory of Section 2 and the results of Section 3 were developed solely for the purposes of demonstrating the margins of safety against unstable fracture. The approach used therein relied on postulated cracks having circumferential lengths of 60, 120 or 180°. It is not suggested that cracks of that size exist because, as this Section will prove, cracks of much shorter lengths are readily detectable.

The safety of the primary coolant system piping at the Indian Point Unit 3 focuses on the ability of leakage monitoring systems to detect leakage size cracks in the piping and the demonstration of their having adequate margins against unstable behavior. The evaluation of this system begins with a description thereof including the code stresses, pipe geometry and operating pressures and temperatures.

The criteria used for the analysis of the primary coolant system piping in this Section is based on that contained in NUREG-1061(16). The approach used is described in the following Sub-Sections.

#### 5-1 PRIMARY COOLANT LOOP PIPING SYSTEM

The primary coolant system provides a continuous flow of coolant through the RPV in order to achieve heat transfer rates greater than that possible by natural convection. The system is composed of 4 loops, similar to the single loop shown in Figure 3-3a. The loops are referred

THIS PAGE IS  
NON-PROPRIETARY

to as loops 31, 32, 33 and 34. In this study, only loop 34 is considered.

The portion of the primary coolant loop piping system that is of interest in this study is limited to the hot leg, cross leg and cold leg piping portions of the loop.

#### 5-1.1 System Description

Following the isometric view of loop 34, shown in Figure 3-3a, the system can be readily explained. Flow from the RPV is via the 29 in. hot leg at a pressure of 2235 psig under normal conditions. The normal operating temperature for the hot leg is 605F. The coolant flows through the hot leg to the steam generator, then via a 31 in. cross leg to the pump and finally thru the 27.5 in. cold leg back to the RPV. The temperatures of the cross and cold legs were taken as 551F and the pressures were assumed to be equal to that of the hot leg.

#### 5-1.2 Piping Code Structural Analysis

Because a stress analysis had already been performed by Westinghouse (17), as part of the design of the NSSS, it was not necessary to perform another. The W stress analysis (WSA) results (17) used herein are taken directly from the stress report. The leak rate computation required by NUREG-1061(16) uses normal operating stresses. To be conservative, for purposes of computing leak rates, the stresses due to dead weight and thermal expansion were neglected and only the pressure term was used.

THIS PAGE IS  
NON-PROPRIETARY

For the crack stability calculations, the seismic or DBE plus thermal plus pressure plus dead weight stresses are required. These could be taken directly from the WSA report, but with some judgement. The WSA stresses are based on the resolved moments about 3 principal axes and an assumption that  $SSE = DBE$ . Because one term is a torsional component, it does not contribute to circumferential crack extension. Thus, it could be removed for computing  $J_{app}$ . Conservatively, the torsional component was not removed. The pressure stress used corresponds to the design pressure. For computational simplicity, the maximum value of the stress along any piping segment is used in lieu of a point by point evaluation. This approach tends to be conservative but greatly simplifies the comprehension of the analysis.

The section properties used for the analysis are given in Table 5-1 and the stresses and their components are given in Table 5-2.

#### 5-2 LEAK DETECTABILITY

NUREG-1061(16) requires the demonstration of the stability of a crack that has a length equal to that which would result in a detectable leakage rate, or "leakage size crack". For this analysis, rates of 1 and 10 gpm, under normal operating loads, were selected as being representative of a leak that is readily detectable using existing methods. At Indian Point 3, both 1 and 10 gpm cracks are detectable within 4 hours(20) and see Appendix D.

### 5-2.1 Circumferential Flaws

The leakage rate computation is conservatively based on the stresses that result from the normal operating pressure (2,235 psi) component(17) alone. The dead weight plus thermal components of stress were conservatively ignored. No dynamic loads are used in developing the stresses for the leak rate computation. It is noted that the lower the stress, the lower the leak rate, and the longer the crack must be in order to have a detectable leak. Leakage rates were computed for a series of crack sizes based on the computed pressure stresses. It was found that cracks having lengths ranging from 6.8 to 7.2 inches correspond to a rate of leakage of 1 gpm. For a 10 gpm rate, the lengths ranged from 11.5 to 12.6 inches. The results are shown in Figure 5-1 and Table 5-3.

### 5-2.2 Longitudinal Flaws

The leakage rates for longitudinal flaws were computed using a hoop stress again conservatively based on a normal operating pressure of 2,235 psi(17). For the range of flaw sizes considered, it was found that a 1 gpm leak rate was attained for cracks having lengths between 3.9 and 4.3 inches. For the 10 gpm rate, the lengths ranged from 7.0 to 7.8 inches. The results are presented in Figure 5-2 and Table 5-3.

### 5-3 CRACK STABILITY, LEVEL D LOADS

This assessment of crack stability for leakage size cracks relies on the small-scale yielding (ssy) theories discussed in Section 4.

#### 5-3.1 Circumferential Flaws

The solution of Equations (4-1) through (4-7) for circumferential flaws was obtained using the computer program, "OYCJT"(18), which performed the necessary iterations on  $K$  to obtain the plastic zone corrected  $K$  values. From the  $K(c+r_y)$  values, the appropriate  $J_{app}$  estimates were determined. This evaluation was performed using the pressure plus dead weight plus thermal plus DBE stresses (17) and the detailed calculations are included in Appendix B.

Crack lengths corresponding to the lengths that cause leak rates of 1 and 10 gpm were considered. For the 1 gpm cases,  $J_{app}$  had a maximum value of 370 in-lb/in<sup>2</sup> for the highest stressed point on the hot leg. The cross leg and cold leg values were found to have maximums of 165 and 130 in-lb/in<sup>2</sup> respectively. For 10 gpm size cracks, the values of  $J_{app}$  ranged from 255 to 790.

The question of material properties poses a continuing dilemma. Current USNRC guidelines(21) for thermally aged stainless steel castings suggest a limit on the value of  $J_{mat} = 3000$ . The value for the margin on crack length was computed using a limit for  $J_{mat} = 3000$ . For that limit, the maximum permitted crack lengths for the hot, cross and cold legs are

25.0, 39.5 and 39.8 inches respectively. Thus, excellent margins on crack length were demonstrated.

To determine the margin on load, the pressure, dead weight and thermal expansion stresses were held constant while the uncertainty in the seismic component was explored. It was found that more than 4 times the DBE load could be tolerated for both 1 and 10 gpm size cracks. This insures an excellent margin of stability based on load.

For the levels of  $J_{app}$  computed using Level D loading and leakage size cracks, it was found that only small amounts of crack extension would occur. Because the loading and amount of crack-tip plasticity are within the ssy regime,  $T_{app}$  is small ( $<6$ ). Thus, no crack instability is indicated for any location. Refer to the results in Appendix B for details of the calculations.

### 5-3.2 Longitudinal Flaws

Crack stability, as evidenced by  $J < J_{Ic}$  and  $J < J_{pzif}$ , was checked using the hoop stress at the pipe wall mid-plane. Upon substituting the appropriate crack lengths ( $2c(10 \text{ gpm})$  plus  $2t$ ) and stresses into Equation (4-8), we find, for the 10 gpm crack, that the plastic zone corrected values of  $J_{app}$  range from 396 to 412 in-lb/in<sup>2</sup>. Because the cracks are longitudinal, it is appropriate to use base metal properties. Again, using a limit of  $J_{mat} = 3000$ , we are insured of crack stability. Having satisfied the fracture toughness criterion, a check for a plastic zone instability failure (PZIF) was made following the methods of Vasquez and

Paris (14).  $J_{pzif}$  was computed using the relation of Equation (4-10) and it was found, that  $J_{app} < J_{pzif}$  thereby satisfying the PZIF criterion. The results are included in Appendix C. These computations were made using the "PZIF"(19) computer code. Larger margins were shown for 1 gpm crack sizes.

Table 5-1 Section Properties

Leg	Dia (in)	t <sub>wall</sub> (in)
Hot	29.0	2.500
Cross	31.5	2.625
Cold	27.5	2.375

Table 5-2 Summary of WSA Results\*

Leg	$\sigma_p$ (psi)	$\sigma_{dw}$ (psi)	$\sigma_{th}$ (psi)	$\sigma_{dbe}$ (psi)	$\sigma_{eff}$ (psi)
Hot	6635.	350.	17150.	4450.	28585.
Cross	6780.	150.	7150.	5550.	19630.
Cold	6624.	250.	7350.	3750.	17979.

$$\sigma_{eff} = \sigma_p + \sigma_{dw} + \sigma_{th} + \sigma_{dbe}$$

\* Values shown equal the maximum at any point along line(17)

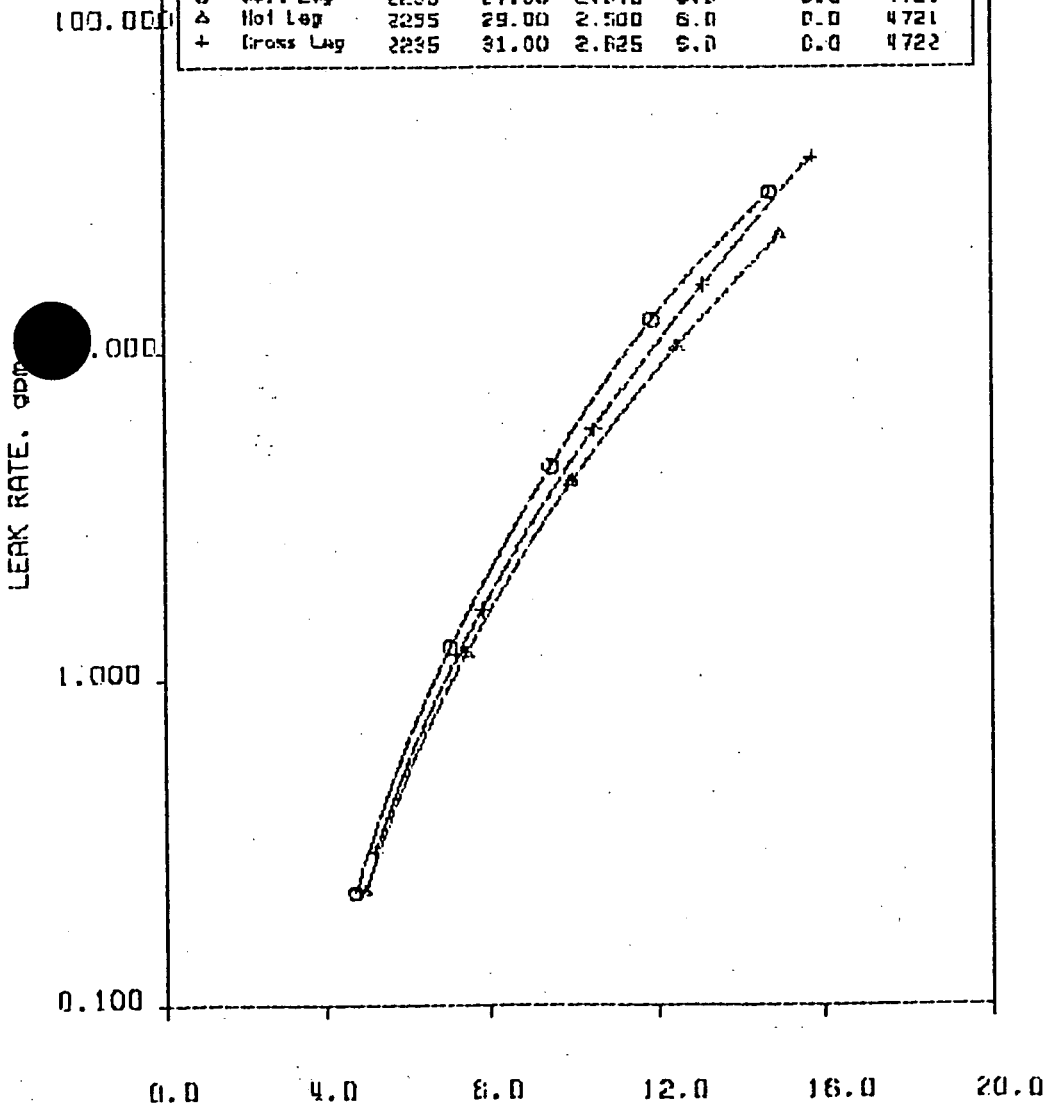
Table 5-3  $J_{app}$  for Leak Rates of 1.0 and 10.0 gpm

Leak Rate (gpm)	Leg	Crack Orientation	Crack Length, $2c$ (inches)	$J_{app}$ in. lb/in <sup>2</sup>
1.0	Hot	LONGITUDINAL	4.5	229
1.0	Cross	LONGITUDINAL	4.5	239
1.0	Cold	LONGITUDINAL	4.5	230
10.0	Hot	LONGITUDINAL	7.8	396
10.0	Cross	LONGITUDINAL	7.8	397
10.0	Cold	LONGITUDINAL	7.8	412
1.0	Hot	CIRCUMFERENTIAL	7.2	370
1.0	Cross	CIRCUMFERENTIAL	7.0	165
1.0	Cold	CIRCUMFERENTIAL	6.8	130
10.0	Hot	CIRCUMFERENTIAL	12.6	790
10.0	Cross	CIRCUMFERENTIAL	11.9	295
10.0	Cold	CIRCUMFERENTIAL	11.5	255

THIS PAGE IS  
NON-PROPRIETARY

PROJECT: INDIAN POINT 3 PRIMARY COOLANT LOOP

SYM	TITLE	P (psi)	D (in)	t (in)	St (ksi)	Sb (ksi)	RUN#
○	Cold Leg	2235	27.50	2.375	6.0	0.0	4720
△	Hot Leg	2255	29.00	2.500	6.0	0.0	4721
+	Cross Leg	2235	31.00	2.625	6.0	0.0	4722



CIRCUMFERENTIAL CRACK LENGTH, 2c, inches

Figure 5-1 Leak Rates for Circumferential Cracks

PROJECT: INDIAN POINT 3 PRIMARY COOLANT LOOP

SYH	TITLE	P (psig)	D (in)	t (in)	Sh (ksi)	RUN#
O	Cold Leg	2235	27.50	2.375	12.9	4723
Δ	Hot Leg	2235	29.00	2.500	12.9	4724
+	Cross Leg	2235	31.00	2.625	13.0	4725

100.000

10.000

1.000

0.100

0.0 4.0 8.0 12.0 16.0 20.0

LONGITUDINAL CRACK LENGTH,  $2c$ , inches

Figure 5-2 Leak Rates for Longitudinal Cracks

## Section 6

### SUMMARY AND CONCLUSIONS

As a result of performing a tearing stability analysis of and developing material property data for the Indian Point Unit 3 Nuclear Plant, a number of conclusions were reached. These conclusions demonstrated that no asymmetric vessel loads can be expected.

The basic tearing stability criteria (6),  $T_{app} < T_{mat}$ , was satisfied unconditionally, for the case of large circumferential cracks under upper-bound loading conditions,  $J_{local}$ , throughout the reactor coolant system. It was demonstrated that under the conditions described by  $J_{local}$  that no crack instabilities would occur for the RCS hot leg, cross leg, or cold leg.

Further, the additional stability criteria, as defined by the structural ductility concepts (4),  $\eta T_{app} < T_{mat}$  was proven for the total applied J-integral,  $J_{app} = J_{local} + J_{abs}$ .

The use of the global crack driving force parameter,  $J_{abs}$ , was shown to be an effective bound to any errors that might occur in a level D or design stress or loads analysis.

The above considerations were shown to be satisfied using lower bound material properties developed for the Indian Point 3 RCS. It was

noted that these material properties varied considerably by product form and whether the crack was located in base or weld metal. It was found that the material tearing resistance (or toughness) of stainless steel piping is an important factor and must be included in any safety analysis.

The earlier analysis of the Indian Point 3 RCS (1) was shown to be too conservative. This observation was based on taking measurements and photographs inside the Indian Point 3 containment and showing that the previously assumed displacement limiting dimensions were excessive.

Using the lbb approach, it was shown that cracks, having lengths which would result in readily detectable leaks, were stable under Code loads (Level D or faulted conditions). Stability was shown for both longitudinal and circumferential cracks. Excellent margins were demonstrated based on crack length criteria and on loads.

The USNRC proposed criteria for alleviation of pipe break postulation (3) was satisfied by this analysis; plus, additional conservatisms were included in the form of structural ductility requirements.

Because no break can occur in the RCS based on the above conclusions, it follows that no large LOCA can be expected. Thus, no asymmetric vessel loads will occur and, accordingly, no vessel restraints are required.

This analysis has met current USNRC criteria (pending) and the material data, previously requested by the USNRC, has been provided. Therefore, it is requested that the requirement to install asymmetric load restraints be eliminated.

1

THIS PAGE IS  
NON-PROPRIETARY

## Section 7

### REFERENCES

1. "Tearing Stability Analysis of the Reactor Coolant System Indian Point 3 Nuclear Power Plant," Fracture Proof Design Corporation Report, May 28, 1981. (PROPRIETARY)
2. "Development of Material Property Data for the Tearing Stability Analysis of the Indian Point 3 Primary Coolant System," FPDC Report 83-104, Rev. 1, September 28, 1983, K. H. Cotter, Paul C. Paris and F. Baradari (PROPRIETARY)
3. "Step-Wise Approach, Leak-Before-Break (LBB) Analysis," Draft USNRC Criteria Dated 11/29/83, prepared by the USNRC Piping Review Committee Staff.
4. "A Critical Review of Methods of Alleviating the Requirement to Postulate Guillotine Type Breaks," Paul C. Paris and Keyren H. Cotter, presented at the CSNI Specialist's Meeting on Leak-Before-Break, September 1 and 2, 1983, Monterey, CA.
5. "Structural Ductility Concepts," Paul C. Paris, FPDC Report 83-76, Rev. 1, May 6, 1983. (PROPRIETARY)
6. "A Treatment of the Subject of Tearing Stability," P. C. Paris, et al., USNRC Report NUREG-0311, August, 1977.
7. "Stability Analysis of Circumferential Cracks in Reactor Piping Systems," H. Tada, P. Paris and R. Gamble, USNRC Report NUREG/CR-0838, February, 1979.
8. "JTIPIPE, A Finite Element Program for Computing the Integrity of Cracked Piping Using Tearing Stability Methodology," FPDC, St. Louis, MO, Ver. 2, Lev 3 (PROPRIETARY).
9. ASME Boiler and Pressure Vessel Code, Section III, Appendix I, 1983.
10. "Material Resistance and Instability Beyond J-Controlled Growth," H. A. Ernst in Elastic-Plastic Fracture: Second Symposium, ASTM STP 803, C. F. Shih and J. P. Gudas, Eds., ASTM, 1983.
11. Indian Point 3 Site Visit Report, K. H. Cotter, FPDC Report 83-77, Sept. 23, 1983.

THIS PAGE IS  
NON-PROPRIETARY

12. Folias, E.S., "A Circumferential Crack in a Pressurized Cylindrical Shell", Intl. J. of Fracture Mechanics, Vol. 3, pp. 1-11, 1967.
13. Erdogan, F. and DeLale, F., "Ductile Fracture of Pipes and Cylindrical Containers with a Circumferential Flaw", ASME J. of Pressure Vessel Technology, Vol. 103, May 1981, pp. 160-168.
14. Vasquez, J. and Paris, P.C., "The Application of the Plastic Zone Instability Criterion to Pressure Vessel Failure", Jornadas Metalurgicas, Sociedad Argentina de Metales, Cordoba, Argentina, Nov. 1970, (also in NUREG/CP-0010, Sept. 1979.)
15. "LKRATE", USNRC computer code for determining leakage rates through cracks in nuclear piping and pressure vessels. Transmitted by M. Boyle, USNRC/SEP to FPDC on Sept. 9, 1982.
16. Report of the USNRC Piping Review Committee, NUREG-1061, Vol. 3, 11/84. 1
17. Structural Analysis of Reactor Coolant Loop/Support System for Indian Point Nuclear Generating Station Unit No. 3, Westinhouse Report SD-109, by Gay, C. W. and Langerud, D. F., Westinghouse Electric Corporation, Pittsburgh, PA 15230.
18. "OYCJT", A Computer Program for Computing Values of  $J_{app}$  for Circumferential Cracks in Pipes, Version 1, Level 5, FPDC, St. Louis, MO.
19. "PZIF", A Computer Program for Computing Values of the  $J_{app}$  and  $J_{pzif}$  for Longitudinal Cracks in Pipes, Version 1, Level 3, FPDC, St. Louis, MO.
20. Indian Point Unit #3 FSAR, Section 6.7 and Appendix 6B, 07/82.
21. Letter, Request for Additional Information, Steven A. Varga to C. A. McNeill, Jr., Dec. 17, 1984.

THIS PAGE IS  
NON-PROPRIETARY

APPENDIX A

JTPIPE

A FINITE ELEMENT PROGRAM FOR COMPUTING  
PIPING SYSTEM CRACK STABILITY PARAMETERS

THIS PAGE IS  
NON-PROPRIETARY

## CONTENTS

- A-1 INTRODUCTION
- A-2 APPROACH
- A-3 ANALYSIS AND IDEALIZATION OF THE STRUCTURE
  - A-3.1 ELEMENT TO STRUCTURAL MATRICES
  - A-3.2 BOUNDARY CONDITIONS
  - A-3.3 COMPLIANCE COMPUTATION AT CRACK SECTION
- A-4 PROGRAM ORGANIZATION
  - A-4.1 NODAL POINT AND ELEMENT DATA INPUT
  - A-4.2 ASSEMBLAGE OF STIFFNESS MATRIX
  - A-4.3 COMPLIANCE CALCULATIONS
  - A-4.4 COMPUTATION OF  $J_{app}$
  - A-4.5 COMPUTATION OF  $T_{app}$

THIS PAGE IS  
NON-PROPRIETARY

## A-1 INTRODUCTION

In NUREG/CR-0838, Tada, et al., applied tearing modulus stability concepts to a selected nuclear reactor piping system geometry and concluded that the piping system was "fracture proof"; that is, unstable ductile crack extension was shown to be unlikely. This was a major breakthrough for the inelastic fracture mechanics analysis of piping. However, in Tada's analysis, the piping system was idealized as a straight beam with simple boundary conditions and the value of  $J_{app}$  was specified. In general, the geometry and the boundary conditions of a nuclear piping system are complicated. To extend the application of Tada's approach to actual piping systems, it became necessary that a finite element program be developed to overcome the structural complexities of typical piping systems and to compute the value of  $J_{app}$  for the case of interest. The JTPIPE program was developed for that purpose.

This Appendix summarizes the capabilities of the current version of the JTPIPE computer program. The detailed theory and the numerical techniques used in JTPIPE are not presented in this Appendix.

The piping systems to be analyzed with JTPIPE can be modeled by combinations of four different types of finite elements. The four element types are:

- a) 3-d straight beam element
- b) 3-d curved beam element
- c) Flexible connection element
- d) Special element

THIS PAGE IS  
NON-PROPRIETARY

## A-2 APPROACH

The program determines the elastic compliance of the piping system at specified locations for use in the crack stability analysis. The location of the maximum compliance is also identified. The computed compliance values are then used to determine principal stiffnesses at each location to be analyzed. From the minimum stiffness at each location, the  $L_{eff}/R$  is determined. The  $L_{eff}/R$  data is stored for post-processing.

Using the aforementioned  $L_{eff}/R$  data,  $J_{app}$  and  $T_{app}$  are computed using Equations (3-3) and (3-5) for each postulated crack location in another program. These latter values are tabulated for a series of circumferential through-wall cracks having included angles of 60 to 300 degrees in 60 degree increments. Alternately, specific angles can be selected. All J vs. T data is saved and later utilized for computer plotting the stability diagram where corresponding material resistance in the form of  $J_{mat}$  vs.  $T_{mat}$  is also included.

## A-3 ANALYSIS AND IDEALIZATION OF THE STRUCTURE

In this section, a brief description of the method of idealization of the structure is presented. The direct stiffness method is used to analyze the structural systems.

## A-3.1 Formulation of Structural Matrices

A piping system is basically a three dimensional frame. It can be idealized as a series of discrete beam (straight or curved) elements, flexible connection

THIS PAGE IS  
NON-PROPRIETARY

elements and special elements. The beam elements are two node elements with six degrees of freedom at each node. The stiffness matrices of the elements are 12 x 12 symmetrical matrices which can be directly formulated from beam theory. After the transformation from the local element coordinate system to the global coordinate system, the total system stiffness matrix can be formed by direct addition of the element matrices according to the index of the degree of freedom. It can be expressed in the following manner:

$$K_{ij} = \sum_{m=1}^N K_{ij}^{(m)} \quad (A-1)$$

where  $K_{ij}$  is the stiffness matrix component of the total system,  $K_{ij}^{(m)}$  is the stiffness matrix component of the  $m^{\text{th}}$  element and  $N$  is the total number of elements in the system.

The external force can be expressed in the form:

$$F_i = \sum_j K_{ij} * U_j \quad (A-2)$$

where  $F_i$  is the external force applied at the  $i^{\text{th}}$  degree of freedom and  $U_j$  is the displacement at the  $j^{\text{th}}$  degree of freedom.

### A-3.2 Boundary Conditions

To simplify the programming problems associated with the specific displacements on the boundary, a spring that is very stiff in comparison with the structure, is assumed to connect the boundary nodal point to a fixed point. If the applied displacement component is zero, the node will be restrained by the stiff

THIS PAGE IS  
NON-PROPRIETARY

spring. If a non-zero displacement component is specified, it can be replaced by equivalent force applied at that nodal point. The equivalent force is evaluated by the specified displacement applied on the stiff spring with the system structure stiffness ignored. Since the spring is much stiffer than the structure, the error introduced is negligible.

Gap elements are included as a feature of the program. These elements may have any one of the principal directions. Displacements limits can be specified in either the +X, +Y or +Z directions.

### A-3.3 Compliance Computation At Cracked Section

In the stability analysis of a through-wall circumferential crack in a piping system, the rotational compliance at the pipe cracked section is required for the computation of the applied tearing modulus,  $T_{app}$ . This is because of the fact that the cracked section of the pipe is idealized as a plastic hinge. The rotational compliance at the pipe cracked section is due to the flexural rigidity of two elastic piping sections joined by the hinged section.

From the total system stiffness, including the boundary conditions, as formulated in Section A-3.1 and A-3.2, the rotational compliance at the pipe cracked section can be obtained by applying unit moments on opposite sides of the hinged section. The principal rotational compliance at that section and the maximum rotational compliance of the selected locations in the piping system are both calculated.

THIS PAGE IS  
NON-PROPRIETARY

## A-4 PROGRAM ORGANIZATION

The computation process in the JTPIPE program is basically divided into five distinct phases plus post-processing.

### A-4.1 Nodal Point And Element Data Input

In this phase, the control information and nodal point geometry data are input and nodal points are generated by the program as required. The indices of the degrees of freedom at each nodal point are established. The element data are input and element groups generated, the element connection arrays and the element coordinate transformation matrices are calculated and all element information is stored in a disc file for use in the second and third phases.

### A-4.2 Assemblage Of System Stiffness Matrix

JTPIPE uses a compacted storage scheme in which the system stiffness matrix is stored as a one-dimensional array. In the second phase, the index of the storage is established, then the system stiffness matrix is assembled and modified to satisfy the boundary conditions.

### A-4.3 Compliance Calculations

In the third phase, the locations of the postulated crack locations desired for the compliance computation, are input. The rotational compliances and minimum stiffnesses at each cracked nodal point is calculated based on the response of the structure to the imposed load. The status of gap elements (open or closed) are

**THIS PAGE IS  
NON-PROPRIETARY**

taken into account at this point. Next, the  $L_{eff}/R$  are calculated and stored for post-processing.

#### A-4.4 Computation of $J_{app}$

$J_{app}$  can be specified by an input value such as  $J_{Ic}$  or an input value for rotation at the cracked section. Alternately,  $J_{app}$  can be determined from the response of the structure. This latter method is the preferred approach but involves considerably longer computer run times.

#### A-4.5 Computation of $T_{app}$

Finally, a post-processor is used to compute  $T_{app}$  for specified crack sizes and  $k$  rotations. The data is displayed in tabular form and is stored on a disk for subsequent post-processing: namely, the generation of J vs. T diagrams.

THIS PAGE IS  
NON-PROPRIETARY

**APPENDIX B**  
**CRACK STABILITY CALCULATIONS**  
**CIRCUMFERENTIAL CRACKS**

**THIS PAGE IS  
NON-PROPRIETARY**

INDIAN POINT 3 PRIMARY LOOP HOT LEG

THERMAL + DEAD WT + SSE

Faxial = 0.            Applied = 0.39870E+08            Poper = 2485. psi  
 Saxial = 0.            Sbending = 21950.            Smem = 6635. psi  
  
 PIPE OD = 34.000            THICKNESS = 2.500            Sflow = 55000. psi  
 ALFA = 6.            ELAS MOD = 0.256E+08            Jic = 1200. in-lb/in\*\*2

CRACK LENGTH, IN	LEAK AREA IN**2	L/Dh	J IN-LB/IN**2	T
4.78	0.032	0.17328E+03	0.22447E+03	0.10304E+01
7.14	0.075	0.10994E+03	0.36328E+03	0.12050E+01
9.48	0.141	0.78098E+02	0.52611E+03	0.14163E+01
11.79	0.232	0.59017E+02	0.71756E+03	0.16649E+01
14.07	0.352	0.46410E+02	0.94239E+03	0.19527E+01
16.31	0.504	0.37551E+02	0.12056E+04	0.22818E+01
18.51	0.692	0.31060E+02	0.15125E+04	0.26546E+01
20.66	0.917	0.26159E+02	0.18687E+04	0.30737E+01
22.75	1.181	0.22375E+02	0.22801E+04	0.35419E+01
24.78	1.483	0.19403E+02	0.27530E+04	0.40620E+01
26.75	1.824	0.17037E+02	0.32940E+04	0.46369E+01
28.64	2.199	0.15132E+02	0.39102E+04	0.52695E+01

\*\*\*\*\* EXCEEDED MAX Japp REQUESTED = NORMAL STOP \*\*\*\*\*

INDIAN POINT 3 PRIMARY LOOP CROSS LEG

THERMAL + DEAD WT + SSE

Faxial = 0.                      Mapped = 0.28074E+08                      Poper = 2485. psi  
 Saxial = 0.                      Sbending = 12050.                      Smem = 6780. psi  
  
 PIPE OD = 36.320                      THICKNESS = 2.625                      Sflow = 55000. psi  
 ALFA = 6.                      ELAS MOD = 0.256E+08                      Jic = 1200. in-lb/in\*\*2

CRACK LENGTH, IN	LEAK AREA IN**2	L/Dh	J IN-LB/IN**2	T
5.14	0.025	0.25175E+03	0.10963E+03	0.48073E+00
7.70	0.059	0.15945E+03	0.17769E+03	0.56141E+00
10.25	0.111	0.11302E+03	0.25729E+03	0.65712E+00
12.78	0.183	0.85161E+02	0.35043E+03	0.76815E+00
15.30	0.280	0.66712E+02	0.45914E+03	0.89511E+00
17.80	0.404	0.53713E+02	0.58556E+03	0.10388E+01
20.28	0.560	0.44156E+02	0.73192E+03	0.12000E+01
22.74	0.751	0.36914E+02	0.90060E+03	0.13798E+01
25.17	0.981	0.31298E+02	0.10941E+04	0.15790E+01
27.58	1.252	0.26865E+02	0.13150E+04	0.17987E+01
29.95	1.568	0.23315E+02	0.15660E+04	0.20400E+01
32.30	1.928	0.20439E+02	0.18502E+04	0.23038E+01
34.61	2.335	0.18085E+02	0.21704E+04	0.25912E+01
36.88	2.788	0.16142E+02	0.25298E+04	0.29033E+01
39.11	3.286	0.14527E+02	0.29317E+04	0.32412E+01
41.29	3.826	0.13176E+02	0.33797E+04	0.36058E+01
43.42	4.404	0.12040E+02	0.38772E+04	0.39984E+01

\*\*\*\*\* EXCEEDED MAX Japp REQUESTED = NORMAL STOP \*\*\*\*\*

INDIAN POINT 3 PRIMARY LOOP COLD LEG

THERMAL + DEAD WT + SSE

Faxial = 0.                      Mapped = 0.17627E+08                      Poper = 2485. psi  
 Saxial = 0.                      Sbending = 11350.                      Smem = 6624. psi  
  
 PIPE OD = 32.260                      THICKNESS = 2.375                      Sflow = 55000. psi  
 ALFA = 6.                      ELAS MOD = 0.256E+08                      Jic = 1200. in-lb/in\*\*2

CRACK LENGTH, IN	LEAK AREA IN**2	L/Dh	J IN-LB/IN**2	T
4.67	0.019	0.27527E+03	0.82984E+02	0.40429E+00
6.99	0.044	0.17411E+03	0.13478E+03	0.47352E+00
9.31	0.083	0.12322E+03	0.19551E+03	0.55549E+00
11.61	0.138	0.92696E+02	0.26671E+03	0.65046E+00
13.90	0.211	0.72494E+02	0.34993E+03	0.75898E+00
16.18	0.306	0.58267E+02	0.44683E+03	0.88169E+00
18.45	0.425	0.47816E+02	0.55911E+03	0.10193E+01
20.70	0.571	0.39902E+02	0.68860E+03	0.11727E+01
22.92	0.748	0.33771E+02	0.83721E+03	0.13427E+01
25.13	0.957	0.28935E+02	0.10069E+04	0.15300E+01
27.32	1.201	0.25067E+02	0.11799E+04	0.17356E+01
29.48	1.481	0.21936E+02	0.14183E+04	0.19604E+01
31.61	1.798	0.19376E+02	0.16645E+04	0.22052E+01
33.71	2.153	0.17265E+02	0.19408E+04	0.24709E+01
35.78	2.543	0.15511E+02	0.22499E+04	0.27584E+01
37.82	2.969	0.14046E+02	0.25943E+04	0.30687E+01
39.81	3.427	0.12814E+02	0.29768E+04	0.34025E+01
41.77	3.913	0.11774E+02	0.34002E+04	0.37609E+01
43.68	4.424	0.10892E+02	0.38676E+04	0.41448E+01

\*\*\*\*\* EXCEEDED MAX Japp REQUESTED = NORMAL STOP \*\*\*\*\*

INDIAN POINT 3 PRIMARY LOOP HOT LEG

THERMAL + DEAD WT + 4xSSE

Faxial = 0.            Mapped = 0.64119E+08            Poper = 2485. psi  
 S axial = 0.            Sbending = 35300.            Smem = 6635. psi  
  
 PIPE OD = 34.000            THICKNESS = 2.500            Sflow = 55000. psi  
 ALFA = 6.            ELAS MOD = 0.256E+08            Jic = 1000. in-lb/in\*\*2

CRACK LENGTH, IN	LEAK AREA IN**2	L/Dh	J IN-LB/IN**2	T
4.52	0.042	0.12368E+03	0.48729E+03	0.22272E+01
6.72	0.099	0.79138E+02	0.78715E+03	0.26028E+01
8.88	0.181	0.56804E+02	0.11390E+04	0.30624E+01
10.97	0.293	0.43466E+02	0.15534E+04	0.36080E+01
12.99	0.435	0.34691E+02	0.20414E+04	0.42438E+01
14.92	0.607	0.28557E+02	0.26143E+04	0.49748E+01
16.76	0.808	0.24096E+02	0.32846E+04	0.58071E+01

\*\*\*\*\* EXCEEDED MAX Japp REQUESTED = NORMAL STOP \*\*\*\*\*

INDIAN POINT 3 PRIMARY LOOP CROSS LEG

THERMAL + DEAD WT + 4xSSE

Faxial = 0.                      Mapped = 0.64450E+08                      Power = 2485. psi  
 Saxial = 0.                      Sbending = 29500.                      Smem = 6780. psi  
  
 PIPE OD = 36.320                      THICKNESS = 2.625                      Sflow = 55000. psi  
 ALFA = 6.                      ELAS MOD = 0.256E+08                      Jic = 1000. in-lb/in\*\*2

CRACK LENGTH, IN	LEAK AREA IN**2	L/Dh	J IN-LB/IN**2	T
4.87	0.043	0.13967E+03	0.38143E+03	0.16568E+01
7.27	0.100	0.89087E+02	0.61567E+03	0.19311E+01
9.62	0.184	0.63683E+02	0.88972E+03	0.22649E+01
11.93	0.300	0.48477E+02	0.12114E+04	0.26593E+01
14.18	0.450	0.38440E+02	0.15888E+04	0.31169E+01
16.37	0.637	0.31396E+02	0.20305E+04	0.36414E+01
18.49	0.860	0.26244E+02	0.25455E+04	0.42367E+01
20.52	1.121	0.22363E+02	0.31433E+04	0.49071E+01

\*\*\*\*\* EXCEEDED MAX Japp REQUESTED = NORMAL STOP \*\*\*\*\*

INDIAN POINT 3 PRIMARY LOOP COLD LEG

THERMAL + DEAD WT + 4xSSE

Faxial = 0.           Applied = 0.35099E+08           Paper = 2485. psi  
 Saxial = 0.           Sbending = 22600.           Smem = 6624. psi  
  
 PIPE OD = 32.260           THICKNESS = 2.375           Sflow = 55000. psi  
 ALFA = 6.           ELAS MOD = 0.256E+08           Jic = 1000. in-lb/in\*\*2

CRACK LENGTH, IN	LEAK AREA IN**2	L/Dh	J IN-LB/IN**2	T
4.53	0.029	0.16969E+03	0.22305E+03	0.10777E+01
6.77	0.069	0.10769E+03	0.36097E+03	0.12605E+01
8.98	0.129	0.76517E+02	0.52279E+03	0.14819E+01
11.17	0.213	0.57843E+02	0.71312E+03	0.17427E+01
13.33	0.323	0.45507E+02	0.93671E+03	0.20447E+01
15.44	0.462	0.36840E+02	0.11986E+04	0.23903E+01
17.52	0.633	0.30492E+02	0.15040E+04	0.27819E+01
19.54	0.839	0.25700E+02	0.18586E+04	0.32223E+01
21.51	1.078	0.22002E+02	0.22684E+04	0.37145E+01
23.42	1.353	0.19099E+02	0.27396E+04	0.42615E+01
25.26	1.660	0.16789E+02	0.32789E+04	0.48663E+01

\*\*\*\*\* EXCEEDED MAX Japp REQUESTED = NORMAL STOP \*\*\*\*\*

**APPENDIX C**  
**CRACK STABILITY CALCULATIONS**  
**LONGITUDINAL CRACKS**

**THIS PAGE IS  
NON-PROPRIETARY**

\*\*\*\*\* CASE = 1 \*\*\*\*\*

LONGITUDINAL CRACK LEAK RATE, LEVEL A  
Leak Rate = 0.1 gpm

Soper                      2c  
11.934                      3.500

LONGITUDINAL CRACK STABILITY, LEVEL D LOADS

Sleak = 11934. psi      Shoop = 14364. psi  
PIPE OD = 34.000 in      THICKNESS = 2.500 in      Sflow = 45000. psi

CRACK LENGTH, IN	RY IN	Ceff	J IN-LB/IN**2	Jpzif
1 8.50	0.000	0.42500E+01	0.15451E+03	0.10874E+04
2 8.50	0.346	0.45956E+01	0.17764E+03	0.11270E+04
3 8.50	0.397	0.46474E+01	0.18131E+03	0.11337E+04
4 8.50	0.406	0.46556E+01	0.18190E+03	0.11347E+04
5 8.50	0.407	0.46569E+01	0.18199E+03	0.11348E+04

\*\*\*\*\* CONVERGENCE ACHIEVED \*\*\*\*\*

\*\*\*\*\* CASE = 2 \*\*\*\*\*

LONGITUDINAL CRACK LEAK RATE, LEVEL A  
Leak Rate = 1.0 gpm

Soper                      2c  
11.934                      4.500

THIS PAGE IS  
NON-PROPRIETARY

LONGITUDINAL CRACK STABILITY, LEVEL D LOADS

Sleak = 11934. psi      Shoop = 14364. psi  
PIPE OD = 34.000 in      THICKNESS = 2.500 in      Sflow = 45000. psi

CRACK LENGTH, IN	RY IN	Ceff	J IN-LB/IN**2	Jpzif
1 9.50	0.000	0.47500E+01	0.18876E+03	0.11454E+04
2 9.50	0.422	0.51722E+01	0.22183E+03	0.11931E+04
3 9.50	0.496	0.52462E+01	0.22805E+03	0.12014E+04
4 9.50	0.510	0.52601E+01	0.22923E+03	0.12029E+04
5 9.50	0.513	0.52628E+01	0.22945E+03	0.12032E+04

\*\*\*\*\* CONVERGENCE ACHIEVED \*\*\*\*\*

HOT

\*\*\*\*\* CASE = 3 \*\*\*\*\*

LONGITUDINAL CRACK LEAK RATE, LEVEL A  
Leak Rate = 10.0 gpm

Soper                      2c  
11.934                    7.800

LONGITUDINAL CRACK STABILITY, LEVEL D LOADS

Sleak = 11934. psi      Shoop = 14364. psi  
PIPE OD = 34.000 in      THICKNESS = 2.500 in      Sflow = 45000. psi

	CRACK LENGTH, IN	RY IN	Ceff	J IN-LB/IN**2	Jprif
1	12.80	0.000	0.64000E+01	0.29305E+03	0.12468E+04
2	12.80	0.656	0.70555E+01	0.36732E+03	0.13487E+04
3	12.80	0.822	0.72217E+01	0.38792E+03	0.13744E+04
4	12.80	0.868	0.72678E+01	0.39376E+03	0.13816E+04
5	12.80	0.881	0.72808E+01	0.39543E+03	0.13836E+04
6	12.80	0.885	0.72846E+01	0.39591E+03	0.13842E+04
7	12.80	0.886	0.72856E+01	0.39604E+03	0.13843E+04

\*\*\*\*\* CONVERGENCE ACHIEVED \*\*\*\*\*

THIS PAGE IS  
NON-PROPRIETARY

NYFA IP3 PRIMARY LOOP PIPING

CROSS LEG LONGITUDINAL CRACK STABILITY

\*\*\*\*\* CASE = 1 \*\*\*\*\*

LONGITUDINAL CRACK LEAK RATE, LEVEL A

Leak Rate = 0.1 gpm

Soper                    2c  
 12.197                  3.500

LONGITUDINAL CRACK STABILITY, LEVEL D LOADS

Sleak = 12197. psi      Shoop = 14658. psi  
 PIPE OD = 36.320 in      THICKNESS = 2.625 in      Sflow = 45000. psi

CRACK LENGTH, IN	RY IN	Ceff	J IN-LB/IN**2	Jpzif
1      8.75	0.000	0.43750E+01	0.16214E+03	0.11370E+04
2      8.75	0.363	0.47377E+01	0.18650E+03	0.11799E+04
3      8.75	0.417	0.47922E+01	0.19038E+03	0.11862E+04
4      8.75	0.426	0.48009E+01	0.19101E+03	0.11872E+04
5      8.75	0.427	0.48023E+01	0.19111E+03	0.11874E+04

\*\*\*\*\* CONVERGENCE ACHIEVED \*\*\*\*\*

\*\*\*\*\* CASE = 2 \*\*\*\*\*

LONGITUDINAL CRACK LEAK RATE, LEVEL A

Leak Rate = 1.0 gpm

Soper                    2c  
 12.197                  4.500

THIS PAGE IS  
 NON-PROPRIETARY

LONGITUDINAL CRACK STABILITY, LEVEL D LOADS

Sleak = 12197. psi      Shoop = 14658. psi  
 PIPE OD = 36.320 in      THICKNESS = 2.625 in      Sflow = 45000. psi

CRACK LENGTH, IN	RY IN	Ceff	J IN-LB/IN**2	Jpzif
1      9.75	0.000	0.48750E+01	0.17639E+03	0.11757E+04
2      9.75	0.439	0.53143E+01	0.23068E+03	0.12456E+04
3      9.75	0.516	0.53910E+01	0.23709E+03	0.12543E+04
4      9.75	0.530	0.54054E+01	0.23831E+03	0.12559E+04
5      9.75	0.533	0.54081E+01	0.23854E+03	0.12562E+04

\*\*\*\*\* CONVERGENCE ACHIEVED \*\*\*\*\*

CROSS

\*\*\*\*\* CASE = 3 \*\*\*\*\*

LONGITUDINAL CRACK LEAK RATE, LEVEL A  
Leak Rate = 10.0 gpm

Soper                      2c  
12.197                      7.800

LONGITUDINAL CRACK STABILITY, LEVEL D LOADS

Sleak = 12197. psi      Shoop = 14658. psi  
PIPE OD = 36.320 in      THICKNESS = 2.625 in      Sflow = 45000. psi

	CRACK LENGTH, IN	RY IN	Ceff	J IN-LB/IN**2	Jpzif
1	13.05	0.000	0.65250E+01	0.34843E+03	0.13813E+04
2	13.05	0.779	0.73044E+01	0.38386E+03	0.14025E+04
3	13.05	0.859	0.73837E+01	0.39363E+03	0.14148E+04
4	13.05	0.881	0.74055E+01	0.39636E+03	0.14182E+04
5	13.05	0.887	0.74116E+01	0.39712E+03	0.14192E+04
6	13.05	0.888	0.74133E+01	0.39734E+03	0.14194E+04

\*\*\*\*\* CONVERGENCE ACHIEVED \*\*\*\*\*

THIS PAGE IS  
NON-PROPRIETARY

\*\*\*\*\* CASE = 1 \*\*\*\*\*

LONGITUDINAL CRACK LEAK RATE, LEVEL A

Leak Rate = 0.1 gpm

Soper                      2c

11.915                    3.500

LONGITUDINAL CRACK STABILITY, LEVEL D LOADS

Sleak = 11915. psi      Shoop = 14343. psi

PIPE OD = 32.260 in      THICKNESS = 2.375 in      Sflow = 45000. psi

CRACK LENGTH, IN	RY IN	Ceff	J IN-LB/IN**2	Jpzif
1      8.25	0.000	0.41250E+01	0.15205E+03	0.10430E+04
2      8.25	0.340	0.44651E+01	0.17544E+03	0.10824E+04
3      8.25	0.392	0.45175E+01	0.17927E+03	0.10884E+04
4      8.25	0.401	0.45260E+01	0.17990E+03	0.10893E+04
5      8.25	0.402	0.45274E+01	0.18000E+03	0.10895E+04

\*\*\*\*\* CONVERGENCE ACHIEVED \*\*\*\*\*

\*\*\*\*\* CASE = 2 \*\*\*\*\*

LONGITUDINAL CRACK LEAK RATE, LEVEL A

Leak Rate = 1.0 gpm

Soper                      2c

11.915                    4.500

THIS PAGE IS  
NON-PROPRIETARY

LONGITUDINAL CRACK STABILITY, LEVEL D LOADS

Sleak = 11915. psi      Shoop = 14343. psi

PIPE OD = 32.260 in      THICKNESS = 2.375 in      Sflow = 45000. psi

CRACK LENGTH, IN	RY IN	Ceff	J IN-LB/IN**2	Jpzif
1      9.25	0.000	0.46250E+01	0.18732E+03	0.11006E+04
2      9.25	0.419	0.50440E+01	0.22129E+03	0.11476E+04
3      9.25	0.495	0.51200E+01	0.22791E+03	0.11561E+04
4      9.25	0.510	0.51348E+01	0.22922E+03	0.11578E+04
5      9.25	0.513	0.51377E+01	0.22948E+03	0.11581E+04
6      9.25	0.513	0.51383E+01	0.22953E+03	0.11582E+04

\*\*\*\*\* CONVERGENCE ACHIEVED \*\*\*\*\*

LONGITUDINAL CRACK LEAK RATE, LEVEL A  
Leak Rate = 10.0 gpm

Soper                      2c  
11.915                      7.800

LONGITUDINAL CRACK STABILITY, LEVEL D LOADS

Sleak = 11915. psi      Shoop = 14343. psi  
PIPE OD = 32.260 in      THICKNESS = 2.375 in      Sflow = 45000. psi

	CRACK LENGTH, IN	RY IN	Ceff	J IN-LB/IN**2	Jpzif
1	12.55	0.000	0.62750E+01	0.29876E+03	0.12147E+04
2	12.55	0.668	0.69433E+01	0.37829E+03	0.13184E+04
3	12.55	0.846	0.71212E+01	0.40157E+03	0.13458E+04
4	12.55	0.898	0.71733E+01	0.40855E+03	0.13539E+04
5	12.55	0.914	0.71889E+01	0.41066E+03	0.13563E+04
6	12.55	0.919	0.71936E+01	0.41130E+03	0.13570E+04
7	12.55	0.920	0.71951E+01	0.41150E+03	0.13572E+04

\*\*\*\*\* CONVERGENCE ACHIEVED \*\*\*\*\*

**APPENDIX D**  
**LEAK DETECTION**

6.7 LEAKAGE DETECTION AND PROVISIONS FOR THE PRIMARY AND AUXILIARY COOLANT LOOPS

6.7.1 Leakage Detection Systems

The leakage detection systems reveal the presence of significant leakage from the primary and auxiliary coolant loops.

6.7.1.1 Design Bases

The General Design Criteria presented and discussed in this section are those which were in effect at the time when Indian Point 3 was designed and constructed. These general design criteria, which formed the bases for the Indian Point 3 design, were published by the Atomic Energy Commission in the Federal Register of July 11, 1967, and subsequently made a part of 10 CFR 50.

The Authority has completed a study of compliance with 10 CFR Parts 20 and 50 in accordance with some of the provisions of the Commission's Confirmatory Order of February 11, 1980. The detailed results of the evaluation of the compliance of Indian Point 3 with the General Design Criteria presently established by the Nuclear Regulatory Commission (NRC) in 10 CFR 50 Appendix A, were submitted to NRC on August 11, 1980, and approved by the Commission on January 19, 1982. These results are presented in Section 1.3.

Monitoring Reactor Coolant Leakage

Criterion: Means shall be provided to detect significant uncontrolled leakage from the reactor coolant pressure boundary. (GDC 16 of 7/11/67)

Positive indications in the Control Room of leakage of coolant from the Reactor Coolant System to the Containment are provided by equipment which permits continuous monitoring of containment air activity and humidity, and of runoff from the condensate collecting pans under the cooling coils of the containment air recirculation units. This equipment provides indication of normal background which is indicative of a basic level of leakage from primary systems and components. Any increase in the observed parameters is an indication of change within the Containment, and the equipment provided is capable of monitoring this change. The basic design criterion is the detection of deviations from normal containment environmental conditions including air particulate activity, radiogas activity, humidity, condensate runoff and in addition, in the case of gross leakage, the liquid inventory in the process systems and containment sump.

These methods are designed to monitor leakage into the Containment atmosphere and as such do not distinguish between identified and unidentified leaks.

### Monitoring Radioactivity Releases

Criterion: Means shall be provided for monitoring the containment atmosphere and the facility effluent discharge paths for radioactivity released from normal operations, from anticipated transients, and from accident conditions. An environmental monitoring program shall be maintained to confirm that radioactivity releases to the environs of the plant have not been excessive. (GDC 17 of 7/11/67)

The containment atmosphere, the plant ventilation exhaust (including exhausts from the Fuel Storage Building, Primary Auxiliary Building, and Waste Holdup Tank Pit), the containment fan-coolers service water discharge, the component cooling loop liquid, the liquid phase of the secondary side of the steam generator, and the condenser air ejector exhaust are monitored for radioactivity concentration during normal operation, anticipated transients and accident conditions.

### Principles of Design

The principles for design of the leakage detection systems can be summarized as follows:

- a) Increased leakage could occur as the result of failure of pump seals, valve packing glands, flange gaskets or instrument connections. The maximum single leakage rate calculated for these types of failures is 50 gpm which would be the anticipated flow rate of water through the pump seal if the entire seal were wiped out and the area between the shaft and housing were completely open.
- b) The leakage detection systems shall not produce spurious annunciation from normal expected leakage rates but shall reliably annunciate increasing leakage.
- c) Increasing leakage rate shall be annunciated in the control room. Operator action will be required to isolate the leak in the leaking system.

For Class I systems located outside the containment, leakage is determined by one or more of the following methods:

- a) For systems containing radioactive fluids, leakage to the atmosphere would result in an increase in local atmospheric activity levels and would be detected by either the plant vent monitor or by one of the area radiation monitors. Similarly leakage to other systems which do not normally contain radioactive

IP3  
FSAR UPDATE

fluids would result in an increase in the activity level in that system.

- b) For closed systems such as the component cooling system, leakage would result in a reduction in fluid inventory.
- c) All leakage would collect in specific areas of the building for subsequent handling by the building drainage systems, e.g., leakage in the vicinity of the residual heat removal pumps would collect in the sumps provided, and would result in operation, or increased operation, of the associated sump pumps.

Details of how these methods are utilized to detect leakage from Class I systems other than the Reactor Coolant System are given in the following sections and summarized in Table 6.7-1.

The Authority has established a program to identify and reduce leakage from systems outside containment that would or could contain highly radioactive fluids during a serious transient or accident (NUREG - 0578). Leak test results for these systems are presented in Table 6.7-2.

#### 6.7.1.2 Systems Design and Operation

Various methods are used to detect leakage from either the primary loop or auxiliary loops. Although described to some extent under each system description, all methods are included here for completeness.

##### Reactor Coolant System

During normal operation and anticipated reactor transients the following methods are employed to detect leakage from the Reactor Coolant System:

##### Containment Air Particulate Monitor

This channel takes continuous air samples from the containment atmosphere and measures the air particulate beta and gamma radioactivity. The samples, drawn outside the Containment, are in a closed, sealed system and are monitored by a scintillation counter - filter paper detector assembly. The filter paper collects all particulate matter greater than 1 micron in size on its constantly moving surface, which is viewed by a hermetically sealed scintillation crystal (NaI) - photomultiplier combination. After passing through the gas monitor, the samples are returned to the Containment.

The filter paper has a 25-day minimum supply at normal speed. The filter paper mechanism, and electromagnetic assembly which controls the filter paper movement, is provided as an integral part of the detector unit.

The detector assembly is in a completely closed housing. The detector output is amplified by a preamplifier and transmitted to the Radiation

IP3  
FSAR UPDATE

Monitoring System cabinet in the Control Room. Lead shielding is provided for the radiogas detector to reduce the background radiation level to where it does not interfere with the detector's sensitivity.

The activity is indicated on meters and recorded by a stripchart recorder. High-activity alarm indications are displayed on the control board annunciator in addition to the radiation monitoring cabinets. Local alarms provide operational status of supporting equipment such as pumps, motors and flow and pressure controllers.

The containment air particulate monitor is the most sensitive instrument of those available for detection of reactor coolant leakage into the Containment. The measuring range of this monitor is given in Section 11.2.

The sensitivity of the air particulate monitor to an increase in reactor coolant leak rate is dependent upon the magnitude of the normal baseline leakage into the Containment. The sensitivity is greatest where baseline leakage is low as has been demonstrated by experience. (See Appendix 6B) Where containment air particulate activity is below the threshold of detectability, operation of the monitor with stationary filter paper would increase leak sensitivity to a few cubic centimeters per minute. Assuming a low background of containment air particulate radioactivity, a reactor coolant corrosion product radioactivity (Fe, Mn, Co, Cr) of approximately 0.4  $\mu\text{c}/\text{cc}$  (a value consistent with little or no fuel cladding leakage), and complete dispersion of the leaking radioactive solids into the containment air, the ~~air particulate monitor~~ is capable of detecting an increase in coolant leakage rate as small as approximately ~~0.25 gpm~~ (100 cc/minute) within twenty minutes after it occurs. If only ten percent of the particulate activity is actually dispersed in the air, leakage rates of the order of 0.25 gpm (1000 cc/minute) are detectable within the same time period.

For cases where baseline reactor coolant falls within the detectable limits of the air particulate monitor, the instrument can be adjusted to alarm on leakage increases from two to five times the baseline value. The containment air particulate monitor together with the other radiation monitors mentioned in this section are further described in Section 11.2

#### Containment Radioactive Gas Monitor

This channel measures the gaseous gamma radioactivity in the Containment by taking the continuous air samples from the containment atmosphere, after they pass through the air particulate monitors, and drawing the samples through a closed, sealed system to a gas monitor assembly.

Each sample is constantly mixed in the fixed, shielded volumes, where it is viewed by Geiger-Mueller tubes. The samples are then returned to the Containment.

IP3  
FSAR UPDATE

The detector is in a completely enclosed housing containing a gamma sensitive Geiger-Mueller tube mounted in a constant gas volume container. Lead shielding is provided to reduce the background radiation level to a point where it does not interfere with the detector's sensitivity. A preamplifier and impedance matching circuit is mounted at the detector.

The detector outputs are transmitted to the Radiation Monitoring System cabinets in the Control Room. The activity is indicated by meters and recorded by a stripchart recorder. High-activity alarm indications are displayed on the control board annunciator in addition to the Radiation Monitoring System cabinets. Local alarms annunciate the supporting equipments' operational status.

The containment radioactive gas monitor is inherently less sensitive (threshold at  $10^{-7}$   $\mu\text{c}/\text{cc}$ ) than the containment air particulate monitor, and would function in the event that significant reactor coolant gaseous activity exists from fuel cladding defects. The measuring range of this monitor is given in Section 11.2. Assuming the design value of reactor coolant gaseous activity (1% fuel cladding defects), the occurrence of a coolant leak of one gpm would double the background in about two hours. For coolant gaseous activity consistent with minimal cladding defects, a one gpm coolant leak would double the background in approximately two minutes. In these circumstances, this instrument is a useful backup to the air particulate monitor.

The containment air particulate and radioactive gas monitors have assemblies that are common to both channels. They are described as follows:

- a) The flow assembly includes a pump unit and selector valves that provide a representative sample (or a "clean" sample) to the detector.
- b) The pump unit consists of:
  - 1) A pump to obtain the air sample
  - 2) A flowmeter to indicate the flow rate
  - 3) A flow control valve to provide flow adjustment
  - 4) A flow alarm assembly to provide low and high flow alarm signals.
- c) Selector valves are used to direct the desired sample to the detector for monitoring and to blow flow when the channel is in maintenance or "purging" condition.
- d) A pressure sensor is used to protect the system from high pressure. This unit automatically closes an inlet and outlet valve upon a high pressure condition.

IP3  
FSAR UPDATE

- e) Purging is accomplished with a valve control arrangement whereby the normal sample flow is blocked and the detector purged with a "clean" sample. This facilitates detector calibration by establishing the background level and aids in verifying sample activity level.
- f) The flow control panel in the Control Room Radiation Monitoring System racks permits remote operation of the flow control assembly. By operating a sample selector on the control panel the containment sample may be monitored.
- g) A sample flow rate indicator is calibrated linearly (from 0 to 14) cubic feet per minute.

Alarm lights are actuated by the following:

- 1) Flow alarm assembly (low or high flow)
- 2) The pressure sensor assembly (high pressure)
- 3) The filter paper sensor (paper drive malfunction)
- 4) The pump power control switch (pump motor on).

#### Humidity Detector

The humidity detection instrumentation offers another means of detection of leakage into the Containment. Although this instrumentation has not nearly the sensitivity of the air particulate monitor, it has the characteristics of being sensitive to vapor originating from all sources within the Containment, including the reactor coolant and steam and feedwater systems. Plots of containment air dew point variations above a base-line maximum established by the cooling water temperature to the air coolers should be sensitive to incremental increases of water leakage to the containment atmosphere on the order of ~~0.25 gpm per~~ degree of dewpoint temperature increase.

The sensitivity of this method depends on cooling water temperature, containment air temperature variation and containment air recirculation rate.

#### Condensate Measuring System

This method of leak detection is based on the principle that, under equilibrium conditions, the condensate flow draining from the cooling coils of the containment air handling units will equal the amount of water (and/or steam) evaporated from the leaking system. Reasonably accurate measurement of leakage from the Reactor Coolant System by this method is possible, because containment air temperature and humidity promote complete

IP3  
FSAR UPDATE

Evaporation of any leakage from hot systems. The ventilation system is designed to promote good mixing within the Containment. During normal operation the containment air conditions will be maintained near 120 F DB and 92 F WB (approximately 36% Relative Humidity) by the fan coolers.

When the water from a leaking system evaporates into this atmosphere, the humidity of the fan cooler intake air will begin to rise. The resulting increase in the condensate drainage rate is given by the equation

$$D = L \left[ 1 - \exp\left(-\frac{Q}{V}t\right) \right]$$

Where:

D = Change in drainage rate after initiation of increased leakage rate (gpm)

L = Change in evaporated leakage rate (gpm)

Q = Containment ventilation rate (CFM)

V = Containment free volume (ft<sup>3</sup>)

t = Time after start of leak (min)

Therefore, if four fan cooler units are operating (Q = 280,000 CFM), the condensation rate would be within 5% of a new equilibrium value in approximately 200 minutes after the start of the leak. ~~Detection~~ of the increasing condensation rate, however, would be possible ~~within 5 to 10 minutes~~.

The condensate measuring device consists essentially of a vertical 6 inch diameter standpipe with a weir cut into the upper portion of the pipe, to serve as an overflow. Each fan cooler is provided with a standpipe which is installed in the drain line from the fan cooler unit. A differential pressure transmitter near the bottom of the standpipe is used to measure the water level. Each unit can be drained by a remote operated valve.

A wide range of flow rates can be measured with this device. Flows less than 1 gpm are measured by draining the standpipe and observing the water level rise as a function of time. Condensate flows from 1 gpm to 30 gpm can be measured by observing the height of the water level above the crest notch of the weir. This water head can be converted to a proportional flow rate by means of a calibration curve. A high level alarm, set above the established normal (baseline) flow, is provided for each unit to warn the operator when operating limits are approached.

All indicators, alarms, and controls are located in the Control Room.

### Component Cooling Liquid Monitors

These channels continuously monitor the component cooling loop of the Auxiliary Coolant System for activity indicative of a leak of reactor coolant from either the Reactor Coolant System, the recirculation loop, or the residual heat removal loop of the Auxiliary Coolant System. Each scintillation counter is located in an in-line well down stream of the component cooling heat exchangers. The detector assembly output is amplified by a preamplifier and transmitted to the Radiation Monitoring System cabinets in the Control Room. The activity is indicated on a meter and recorded by a two-point recorder. High activity alarm indications are displayed on the control board annunciator in addition to the Radiation Monitoring System cabinets.

The measuring range of this monitor is given in Section 11.2.

### Condenser Air Ejector Gas Monitor

This channel monitors the discharge from the air ejector exhaust header of the condensers for gaseous radiation which is indicative of a primary to secondary system leak. The gas discharge is routed to the turbine roof vent. On high radiation level alarm, this gas discharge is diverted to the Containment.

The detector output is transmitted to the Radiation Monitoring System cabinets in the Control Room. The activity is indicated by a meter and recorded by a two-point recorder. High activity alarm indications are displayed on the control board annunciator in addition to the Radiation Monitoring cabinets.

A remote indicator panel, mounted at the detector location, indicates the radiation level and high radiation alarm.

A gamma sensitive Geiger-Mueller tube is used to monitor the gaseous radiation level. The detector is inserted into an in-line fixed volume container which includes adequate shielding to reduce the background radiation to where it does not interfere with the detector's maximum sensitivity. The sensitivity of this monitor is given in Section 11.2.

### Steam Generator Liquid Sample Monitor

This channel monitors the liquid phase of the secondary side of the steam generator for radiation, which would indicate a primary-to-secondary system leak, providing backup information to that of the condenser air ejector gas monitor. Samples from the bottom of each of the four steam generators are mixed to a common header and the common sample is continuously monitored by a scintillation counter and holdup tank assembly. Upon indication of a high radiation level, each steam generator is individually sampled in order

to determine the source. This sampling sequence is achieved by manually selecting the desired unit to be monitored and allotting sufficient time for sample equilibrium to be established (approximately 1 minute).

The sensitivity range of this monitor is given in Table 11.2-7.

A photomultiplier tube - scintillation crystal (NaI) combination, mounted in a hermetically sealed unit, is used to monitor liquid effluent activity. Lead shielding is provided to reduce the background level so it does not interfere with the detector's maximum sensitivity. The in-line, fixed-volume container is an integral part of the detector unit.

Personnel can enter the Containment and make a visual inspection for leaks. The location of any leak in the Reactor Coolant System would be determined by the presence of boric acid crystals near the leak. The leaking fluid transfers the boric acid crystals outside the Reactor Coolant System and the evaporation process leaves them behind.

If an accident involving gross leakage from the Reactor Coolant System occurred it could be detected by the following methods:

#### Pump Activity

During normal operation only one charging pump is operating. If a gross loss of reactor coolant to another closed system occurred which was not detected by the methods previously described, the speed of the charging pump would indicate the leakage.

The leakage from the reactor coolant will cause a decrease in the pressurizer liquid level that is within the sensitivity range of the pressurizer level indicator. The speed of the charging pump will automatically increase to try to maintain the equivalence between the letdown flow and the combined charging line flow and flow across the reactor coolant pump seals. If the pump reaches a high speed limit, an alarm is actuated.

A break in the primary system would result in reactor coolant flowing into the Containment, reactor vessel, and/or recirculation sumps. Gross leakage to these sumps would be indicated by the frequency of operation of the containment or recirculation pumps. Since the building floor drains preferentially to the containment sump, the operating frequency of the containment sump pumps would be more likely to indicate the leak than the operating frequency of the recirculation or reactor vessel sump pumps.

The ~~containment sump~~ contains two (2) ~~level indicators~~ each consisting of a column containing five (5) level switches which indicate a vertical array of five (5) lights on the control room supervisory panel. Two (2) out of the five (5) switches on each level indicator measure level within the sump.

IP3  
FSAR UPDATE

In addition an overflow alarm provides an annunciated alarm on the control room supervisory panel if the level in the sump reaches the containment floor. The recirculation sump contains two (2) level indicators, each consisting of a column containing five (5) level switches which indicate a vertical array of five (5) lights on the control room supervisory panel. One (1) switch on one indicator measures level within the sump while three (3) switches on the other indicator measure level within the sump.

The reactor vessel sump contains a level indicator which annunciates two (2) alarms on the control room supervisory panel. These alarms will annunciate at different levels when the sump accumulates with water prior to the level reaching the in-core instrumentation tubing for the reactor vessel. In addition, when the first sump pump starts, an indicating light will illuminate on the control room supervisory panel.

The containment sump contains two (2) sump pumps which are actuated by separate pump float switches. These pumps discharge the water to the waste holdup tank outside Containment. Located on this discharge line outside containment is the flow meter and totalizer, which indicates on the Primary Auxiliary Building waste disposal panel the flow from the pumps and a cumulative measure of the amount of water being discharged from Containment. The cumulative volume is trended by the control room operators to identify any abnormal increases in leakage on a daily basis. In addition, indicating lights on the waste disposal panel indicate when the containment sump pumps are running. This panel is periodically operated and monitored by the auxiliary operator who reports directly to the control room operator.

The recirculation sump contains redundant level indication. Loss of both of these level indications for more than seven days requires a plant shutdown in accordance with Technical Specifications. The sump pumps, which discharge into the Reactor Coolant System, are required for a LOCA and require an immediate plant shutdown if they become inoperable.

The reactor vessel sump contains a level indicator which annunciates at two separate levels. In addition, the running of the first sump pump indicates in the Control Room. At the present time during normal plant operation, there is no means to test operability of either the level indication or pumps since this sump is normally maintained dry.

The containment sump contains redundant level indication. Loss of both of these level indications for more than seven days requires a plant shutdown in accordance with the Technical Specifications. Even if both level indications were operable, the level probe at the top of the sump would still provide an annunciated alarm. In addition, the sump pumps indicating lights and the flow meter/totalizer on the waste disposal panel outside containment provide back up indication of conditions occurring in the sump. Both pumps operate independently, but should they both become inoperable, a containment entry would be performed to attempt to make any necessary repairs. If the pumps could not be made operable, continued plant operation

would be considered after a complete evaluation of the leakage rate, waste holdup tank capacity and source of the leakage.

### Liquid Inventory

Gross leaks might be detected by unscheduled increases in the amount of reactor coolant makeup water which is required to maintain the normal level in the pressurizer.

A large tube side to shell side leak in the non-regenerative (letdown) heat exchanger would result in reactor coolant flowing into the component cooling water and a rise in the liquid level in the component cooling water surge tank. The operator would be alerted by a high water alarm for the surge tank and high radiation and temperature alarms actuated by monitors at the component cooling water pump suction header. In addition a low flow alarm would be actuated by a monitor on the outlet line of the Chemical and Volume Control System from the non-regenerative heat exchanger.

A high level alarm for the component cooling water surge tank and high radiation and temperature alarms actuated by monitors at the component cooling pump suction header could also indicate a thermal barrier cooling coil rupture in a reactor coolant pump. However, in addition to these alarms, high temperature and high flow on the component cooling outlet line from the pump would activate alarms.

Gross leakage might also be indicated by a rise in the normal containment and/or recirculation sump levels. High level in either of these sumps is indicated in the Control Room by indicating lights. Since the building floor drains preferentially to the containment sump, the containment sump level transmitter would most likely be actuated prior to the level transmitter in the recirculation sump.

The ~~maximum leakage rate~~ from an unidentified source that will be ~~permitted~~ during normal operation is ~~1 gpm~~.

Leakage directly into the Containment indicates the possibility of a breach in the coolant envelope. The limitation of 1 gpm for a source of leakage not identified is sufficiently above the minimum detectable leakage rate to provide a reliable indication of leakage. The 1 gpm limit is well below the capacity of one coolant charging pump (98 gpm).

The relationship between leak rate and crack size has been studied in detail in WCAP-7503(1), Revision 1, February 1972. This report includes the following information:

- 1) The length of a through-wall crack that would leak at the rate of the proposed limit, as a function of wall thickness.
- 2) The ratio of that length to the length of a critical through-wall crack, based on the application of the principles of fracture mechanics.
- 3) The mathematical model and data used in such analyses.

Leak rate detection is not relied upon for assuring the integrity of the primary system pressure boundary during operation. The conservative approach which is utilized in the design and fabrication of the components which constitute the primary system pressure boundary together with the operating restrictions which are imposed for system heatup and cooldown give adequate assurance that the integrity of the primary system pressure boundary is maintained throughout plant life. The periodic examination of the primary pressure boundary via the in-service inspection program (specified in the Technical Specifications) will physically demonstrate that the operating environment will have no deleterious effect on the primary pressure boundary integrity.

The maximum unidentified leak rate of 1 gpm which is permitted during normal operation is well within the sensitivity of the leak detection systems incorporated within the containment, and it reflects good operating practice based on operating experience gained at other PWR plants. Detection of leakage from the primary system directs the operator's attention to potential sources of leakage such as valves, and permits timely evaluation to ensure that any associated activity release does not constitute a public hazard, that the reactor coolant inventory is not significantly affected and that the leakage is well within the capability of the containment drainage system.

#### Residual Heat Removal Loop

The residual heat removal loop removes residual and sensible heat from the core and reduces the temperature of the Reactor Coolant System during the second phase of plant shutdown.

During normal operation the containment air particulate and radioactive gas monitors, the humidity detector and the condensate measuring system provide means for detecting leakage from the section of the residual heat removal loop inside the Reactor Containment. These systems have been described previously in this section (see description of leak detection from the Reactor Coolant System). Leakage from the residual heat removal loop into the component cooling water loop during normal operation would be detected outside the Containment by the component cooling loop radiation monitor (see analysis of detection of leakage from the Reactor Coolant System in this section).

APPENDIX 6B

PRIMARY SYSTEM LEAK DETECTION INTO CONTAINMENT VESSEL

1.0 INTRODUCTION

Small leaks developed in the primary system pressure boundary could be detected by several continuously recording instruments available to the plant operators. The most sensitive of these detectors is the radioactive air particulate monitor which continuously samples the air in the containment cooling system. The purpose of the containment cooling system is to maintain proper ambient temperatures for equipment in the containment vessel. This system takes air from the upper elevations of the vessel and recirculates it through cooling coils on the suction side of the supply fan. This air is then discharged at a rate of 40,000 cfm. The turnover rate of air in the containment vessel as a result of this system is approximately once every hour. By sampling air from the discharge of the containment cooling system supply fan, leak rates as small as 0.3 gph (20 cc/minute) could be detected.

Another detector, the radiogas monitor, sampling air from the same position as the air particulate monitor, continuously analyzes air from the containment cooling system for gaseous radioactivity. This monitor is capable of detecting a leak rate of about 100 gph (6500 cc/minute).

In addition to measuring changes in the radioactivity of the containment vessel, dew point sensors continuously sample the air from the suction side of the containment cooling system supply fans. These instruments could detect a primary coolant leak rate of approximately 1 gph (250 cc/minute) by measuring changes in the moisture content of the containment vessel.

By the use of the above instruments, plant operators could continuously monitor the containment vessel for primary system leakage and take any steps necessary to operate the facility safely. Measurements made by the New York University Medical Center, Institute of Environmental Medicine, have shown that the samples analyzed by these instruments are representative of the containment vessel and that samples taken manually to back up these detectors were accurate to within a factor of 2.

Other methods for detecting and locating primary system leakage include visual inspection for escaping steam or water, boric acid crystal formation, component and primary relief tank levels, hydrogen concentration and radioactivity, containment sump level, and manually taken samples for tritium radioactivity in condensed moisture from the containment vessel.

1.0

SAMPLE CALCULATIONS

To determine the leak rate utilizing measurements from the instrumentation discussed in Paragraph 1.0, the following method must be applied:

Assumptions

The calculations are based on the assumption that:

- 1) Uniform mixing in the Containment occurs within one hour after initiation of the leak when one cooling fan is in service at a flow of 40,000 cfm.
- 2) The smallest significant change for the radiogas monitor which reflects the presence of a leak is 1 count per second (cps), which is equivalent to an increase in activity of  $3 \times 10^{-7}$   $\mu\text{c}/\text{cc}$  of air.
- 3) The smallest significant change for the particulate monitor which reflects the presence of a leak is 8 cps, which is equivalent to an increase in activity of  $8 \times 10^{-9}$   $\mu\text{c}/\text{cc}$  of air.
- 4) A period of eight hours is used to evaluate these changes, which provides time for checking the instrumentation and determining the cause of the leak. This eight hour period is predicated for determining the magnitude of small leaks, large leaks would be evaluated much sooner.

Basic Data Used for Calculations

- 1) Containment volume:  $1.8 \times 10^6$   $\text{ft}^3$  ( $5.05 \times 10^{10}$  cc)
- 2) Normal containment environment:
  - a) Average temperature: 120 F
  - b) Dewpoint temperature: 70 F
  - c) Water content: 0.016 lbs of water/lb of dry air
- 3) Normal radioactivity in the containment cooling system:
  - a) Radiogas: 2.5 cps ( $7.5 \times 10^{-7}$   $\mu\text{c}/\text{cc}$ )
  - b) Particulate: 16 cps ( $1.6 \times 10^{-3}$   $\mu\text{c}/\text{cc}$ )
- 4) Normal primary coolant radioactivity after one hour:
  - a) Radiogas:  $5 \times 10^{-3}$   $\mu\text{c}/\text{ml}$  of  $\text{H}_2\text{O}$
  - b) Particulate:  $5 \times 10^{-2}$   $\mu\text{c}/\text{ml}$  of  $\text{H}_2\text{O}$

Calculations

Dewpoint

The smallest leak that can be detected will result in an increase in the dewpoint reading from 70 F to 74 F. The water content of the containment atmosphere at a 74 F dewpoint would be 0.018 lbs of water per lb of dry air.

Letting

- X = the leak rate into the Containment in gph
- $h_a$  = the water content at a dewpoint of 70 F
- $h_b$  = the water content at a dewpoint of 74 F
- $V_c$  = the volume of the Containment in  $ft^3$
- $\rho_a$  = the density of the containment atmosphere in  $lb/ft^3$
- t = the evaluation period, and
- k = 8.3 lbs/gallon for water

Then:

$$X = (h_b - h_a) V_c \rho_a / tk$$

or

$$X = (0.018 - 0.016)(1.8 \times 10^6)(0.081 \times 109/121)/(8)(8.3)$$

$$= 3.95 \text{ gph (100 gpd)}$$

Radiogas Activity

For the smallest significant change for the radiogas monitor (1 cps) the corresponding leak rate could be determined as follows:

Let

- Y = the leak rate into the Containment in gph
- $C_g$  = the radiogas activity increase ( $3.0 \times 10^{-7} \mu\text{c/cc}$  of air)
- $V_c$  = the volume of the Containment in cc
- t = the evaluation period
- $I_g$  = the primary coolant radioactivity after one hour, and
- k =  $3.8 \times 10^3$  ml/gal for water

Then:

$$Y = C_g V_c / t I_g k$$

or

$$Y = (3.0 \times 10^{-7})(5.05 \times 10^{10})/(8)(5 \times 10^3)(3.8 \times 10^3)$$

$$= 99.8 \text{ gph (2400 gpd)}$$

Particulate Activity

For the smallest significant change for the particulate monitor (8 cps) the corresponding leak rate could be determined as follows:

Let

- Z = the leak rate into the Containment in gph
- $C_p$  = the particulate activity increase ( $8 \times 10^{-9}$   $\mu\text{c}/\text{cc}$  of air)
- $V_c$  = the volume of the Containment in cc
- t = the evaluation period
- $I_p$  = the primary coolant radioactivity after one hour, and
- k =  $3.8 \times 10^3$  ml/gal for water

Then:

$$Z = C_p V_c / t I_p k$$

or

$$Z = (8 \times 10^{-9})(5.05 \times 10^{10}) / (8)(5 \times 10^{-2})(3.8 \times 10^3) \\ = 0.265 \text{ gph (6 gpd).}$$

6/11  
~~6/11~~



**PROP**

# PROPRIETARY INFORMATION

## NOTICE

THE ATTACHED DOCUMENT MAY CONTAIN "PROPRIETARY INFORMATION" AND SHOULD BE HANDLED AS NRC "OFFICIAL USE ONLY" INFORMATION. IT SHOULD NOT BE DISCUSSED OR MADE AVAILABLE TO ANY PERSON NOT REQUIRING SUCH INFORMATION IN THE CONDUCT OF OFFICIAL BUSINESS AND SHOULD BE STORED, TRANSFERRED, AND DISPOSED OF BY EACH RECIPIENT IN A MANNER WHICH WILL ASSURE THAT ITS CONTENTS ARE NOT MADE AVAILABLE TO UNAUTHORIZED PERSONS.

COPY NO. \_\_\_\_\_

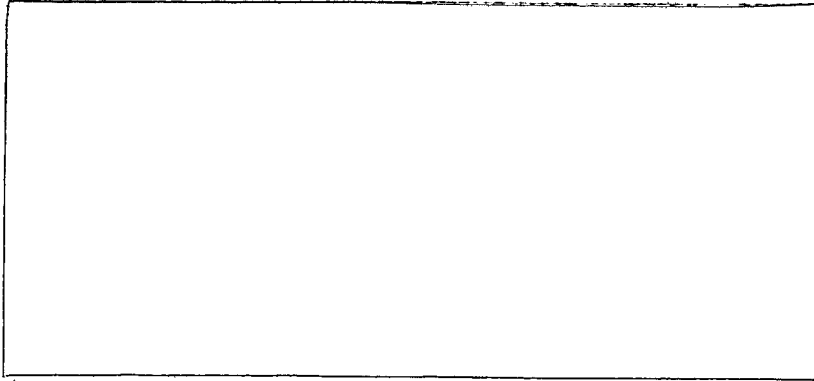
DOCKET NO. \_\_\_\_\_

CONTROL NO. \_\_\_\_\_

REPORT NO. \_\_\_\_\_

REC'D W/LTR DTE \_\_\_\_\_

# PROPRIETARY INFORMATION



**— NOTICE —**

THE ATTACHED FILES ARE OFFICIAL RECORDS OF THE DIVISION OF DOCUMENT CONTROL. THEY HAVE BEEN CHARGED TO YOU FOR A LIMITED TIME PERIOD AND MUST BE RETURNED TO THE RECORDS FACILITY BRANCH 016. PLEASE DO NOT SEND DOCUMENTS CHARGED OUT THROUGH THE MAIL. REMOVAL OF ANY PAGE(S) FROM DOCUMENT FOR REPRODUCTION MUST BE REFERRED TO FILE PERSONNEL.

DEADLINE RETURN DATE \_\_\_\_\_  
\_\_\_\_\_  
\_\_\_\_\_  
\_\_\_\_\_

RECORDS FACILITY BRANCH

11

